CZECH TECHNICAL UNIVERSITY IN PRAGUE

Faculty of Nuclear Sciences and Physical Engineering

Department of Solid State Engineering

BACHELOR THESIS

Quantum hydrodynamics described by Lagrangian formalism

Author: Veronika Rečková

Supervisor: Mgr. Jaroslav Hamrle, Ph.D.

Academic year: 2021/2022

ČESKÉ VYSOKÉ UČENÍ TECHNICKÉ V PRAZE
FAKULTA JADERNÁ A FYZIKÁLNĚ INŽENÝRSKÁ
Katedra inženýrství pevných látek

ZADÁNÍ BAKALÁŘSKÉ PRÁCE

Student:	**Veronika Rečková**
Studijní program:	**Aplikace přírodních věd**
Obor:	**Inženýrství pevných látek**
Akademický rok:	**2021/2022**
Název práce: *(česky)*	**Kvantová hydrodynamika popsaná pomocí Lagrangeova formalizmu**
Název práce: *(anglicky)*	***Quantum hydrodynamics described by Lagrangian formalism***

Pokyny pro vypracování:

Kvantová hydrodynamika charakteruzuje pohyb mnoha-elektronového systému blízko základního stavu. Tento formalizmus popisuje vývoj elektronové hustoty v čase a prostoru, v závislosti na excitačním poli (např. světelný puls), a typicky se používá k popisu chování nerovnovážných elektronů v kovových nanometrových nanočásticích, obsahujících řádově tisíce atomů, kde DFT přístup již nelze použít pro výpočetní obtížnost problému. Cílem bakalářské práce je seznámit se s přístupy řešení v kvantové hydrodynamice pomocí Lagrangeova formalizmu, speciálně pak popsat chování elektronové hustoty v kovové nanočástici při excitaci světelnou vlnou.

Při řešení postupujte podle následujících bodů.

I. Rešeršní a obecná část
   1) Nastudování formalismu kvantové hydrodynamiky pomocí Lagrangeova formalizmu.
   2) Popis jednotlivých členů v Lagrangianu.
   3) Odvození pohybových rovnic kvantové hydrodynamiky z Lagrangeova formalismu.

II. Výpočetní část
   4) Výpočet pohybových rovnic elektronové hustoty pro kulovou kovovou nanočástici. Tento výpočet bude založen na tzv. ansatz přístupu (znalosti předpokládaného tvaru řešení).

5) Určení základního stavu elektronové hustoty. Určení odezvy elektronové hustoty na excitující světelné záření, např. pro dipolový a dýchací (breathing) mód.
6) Porovnání výsledků získaných pomocí řesení kvantového hydrodynamického modelu s výsledky klasické lokální elektrodynamiky, aplikované na jednoduchý plazmonický systém, např. získané pomocí vhodných numerických simulací dle nástrojů dostupných na pracovišti konzultanta.

Doporučená literatura:

[1] J. Hurst et al: Phys. Rev. B 98 (2018) article # 134439.
[2] H.M. Baghramyan et al: Phys. Rev. X 11 (2021) article # 011049.
[3] S. Maier: Plasmonics: fundamentals and applications. Springer, New York 2007.
[4] M. Bonitz et al: Quantum hydrodynamics for plasmas—Quo vadis? Phys. Plasmas 26 (2019) article # 090601.

Jméno a pracoviště vedoucího práce:
Mgr. Jaroslav Hamrle, Ph.D., Katedra inženýrství pevných látek, Fakulta jaderná a fyzikálně inženýrská, ČVUT v Praze.

Jméno a pracoviště konzultanta:
Ing. Pavel Kwiecien, Ph.D., Katedra fyzikální elektroniky, Fakulta jaderná a fyzikálně inženýrská, ČVUT v Praze.

Datum zadání bakalářské práce: 21. 10. 2021

Termín odevzdání bakalářské práce: 7. 7. 2022

Doba platnosti zadání je dva roky od data zadání.

.....
garant

.....
vedoucí katedry

ČESKÉ VYSOKÉ UČENÍ TECHNICKÉ V PRAZE
Fakulta jaderná a fyzikálně inženýrská
-1-

.....
děkan

V Praze dne 21. 10. 2021

Declaration

I declare that I carried out this bachelor thesis independently, and only with the cited sources.

In Prague, 7.7.2022

.....
Veronika Rečková

I would like to express my greatest gratitude to my thesis supervisor Mgr. Jaroslav Hamrle, Ph.D., for his helpful guidance, insightful advice and endless patience. I would also like to thank my parents and Juraj for their incredible support and encouragement all throughout my studies.

Title: **Quantum hydrodynamics described by Lagrangian formalism**

Author: Veronika Rečková

Department: Department of Solid State Engineering

Supervisor: Mgr. Jaroslav Hamrle, Ph.D., Department of Solid State Engineering

Consultant: Ing. Pavel Kwiecien, Ph.D., Department of Physical Electronics

Abstract: This thesis focuses on quantum hydrodynamics as a method of modelling dynamics of electrons in a golden nanoparticle. In the first part of the thesis, we derive the quantum hydrodynamic equations from the Lagrangian density. We choose an expected solution (ansatz) for the electron density, parametrized by the spillout of the electrons at the surface of nanoparticle $\sigma(t)$ and displacement of center of mass of the electrons relative to fixed ion background $d(t)$. Subsequently, we integrate the Lagrangian density over space in order to obtain the Lagrangian. Using the Euler-Lagrange method, we obtain equations of motion with two dynamic variables $\sigma(t)$ and $d(t)$. We determine the ground state and investigate eigenfrequencies of oscillations of $\sigma(t)$ and $d(t)$. Furthermore, we investigate oscillations after applying damping and alternating external electric field, which models external illumination of the nanoparticle. In the final part of the thesis, we determine and visualize the distribution of the current density of electrons.

Key words: nanoparticle, quantum hydrodynamics, dipole mode, breathing mode, Lagrangian, electron density, ansatz

Contents

Introduction

There are numerous different approaches to the many-electron problem. The most commonly applied approach is the Density-functional theory (DFT). In DFT, charge density is used to express the energy of non-interacting pseudoelectrons (Kohn-Sham equations), and calculation of wavefunctions of these pseudoelectrons is required [1]. However, this approach is sustainable only for a periodic system or for a smaller number of electrons in the system. If we want to model a nanoparticle with a larger number of electrons, in the order of 10^3 or higher, DFT becomes computationally demanding.

In this thesis, we are going to model electron dynamics in a golden nanoparticle with radius of 1 nm and we are going to apply a different approach, which models the electron density in a fluid-like fashion. In this approach, we do not investigate wavefunctions of electrons, rather the electron density. This approach is called Quantum hydrodynamics (QHD) and has found different applications over the past years, for example in warm dense matter, electrons in metals and electron-hole plasmas in semiconductors. [2]

The jumping-off point in our theoretical description of a golden nanoparticle are the QHD equations, which consist of the motion equation, continuity equation and Poisson equation [3]. The Lagrangian density can be derived from these equations and contains the same information - the Lagrangian density and QHD equations are equivalent. We are going to solve the equations using an expected solution (ansatz) for the charge density of electrons.

This thesis is dedicated to a detailed derivation and subsequent solution of equations describing electron dynamics in a golden nanoparticle. In the final part of the thesis, we are going to focus on placing the nanoparticle in an alternating external electric field and investigating the oscillations of two dynamic variables: spillout of the electrons at the surface of nanoparticle $\sigma(t)$ and displacement of center of mass of the electrons relative to fixed ion background $d(t)$. Lastly, we are going to visualize the distribution of the electronic current density in the nanoparticle.

Chapter 1

Quantum Hydrodynamic Equations

1.1 Derivation of terms in the Lagrangian density

We are going to study electron dynamics in a spherical golden nanoparticle with radius R, containing N free electrons. The jellium approximation will be used, where the positively charged ions form a uniform charge background with a density of n_i inside the particle and zero outside. In this thesis, atomic units are used (namely: $\hbar = 1$, $e = 1$ (elementary charge), $a_o = 1$ (Bohr radius), $m_e = 1$ (electron mass)). Thus, the constant $\frac{1}{4\pi\epsilon_0}$ is also equal to 1. The conversion between nanometers and atomic units of length is 1 nm $\approx 18.897\,\mathrm{AU}$ of length, the conversion between electronvolts and atomic units of energy is $1\,\mathrm{eV} \approx 0.03675\,\mathrm{AU}$ of energy.

In order to derive the QHD (quantum hydrodynamic) equations [3, 4], the Lagrangian density must be determined first. The Lagrangian density is a function of 3 scalar fields: electron density $n(\mathbf{r}, t)$, the Hartree potential $V_h(\mathbf{r}, t)$ and the phase function $S(\mathbf{r}, t)$, related to mean velocity of electrons $\mathbf{u}(\mathbf{r}, t) = \nabla S$.

We are going to define the Lagrangian density in the following way [3, 4]:

$$\begin{aligned}\mathscr{L} = n\left(\frac{\partial S}{\partial t} + \frac{(\nabla S)^2}{2}\right) + \frac{3}{10}\left(3\pi^2\right)^{2/3} n^{5/3} \\ - \frac{3}{4\pi}\left(3\pi^2\right)^{1/3} n^{4/3} - \frac{(\nabla V_h)^2}{8\pi} + (n_i - n)\, V_h.\end{aligned} \tag{1.1}$$

The first term in the Lagrangian density represents kinetic energy of the center of mass of electrons (movement of electrons as a continuum):

$$n\left(\frac{\partial S}{\partial t} + \frac{(\nabla S)^2}{2}\right). \tag{1.2}$$

The physical meaning of this term will become clear in section 1.2 where we derive the QHD equations, as the corresponding term in the equation of motion derived from the Lagrangian density will be (atomic units)

$$\frac{\partial \mathbf{u}}{\partial t} + \mathbf{u} \cdot \nabla \mathbf{u},$$

a term that describes time derivative of momentum of electrons as a continuum.

The second term in the Lagrangian density accounts for internal kinetic energy of electrons, commonly referred to as Fermi pressure [3, 4], and can be derived in the following way:

$$T = 2\sum_{\mathbf{k},|\mathbf{k}|\leq k_F} \frac{\hbar^2 k^2}{2m} = 2\frac{V}{8\pi^3}\int_{|\mathbf{k}|\leq k_F} \frac{\hbar^2 k^2}{2m} d\mathbf{k} = 2\frac{V}{8\pi^3} 4\pi \int_0^{k_F} \frac{\hbar^2 k^2}{2m} k^2 dk$$
$$= \frac{V}{\pi^2}\frac{\hbar^2}{2m}\frac{1}{5}{k_F}^5 = \frac{V}{\pi^2}\frac{\hbar^2}{10m}(3\pi^2 n)^{5/3}.$$

Kinetic energy is multiplied by a factor of 2, because each k-state allows for two electron states with opposite spin. This derivation of internal kinetic energy holds for electron gas in a box. Our assumption is that the equation also holds locally, for electron density as a function of position and time $n(\mathbf{r}, t)$. Kinetic energy T is then divided by volume V, as the term in the Lagrangian density must correspond to energy density:

$$\frac{T}{V} = \frac{3}{10}(3\pi^2)^{2/3}\frac{\hbar^2}{m}n^{5/3}.$$

Thus, the second term in the Lagrangian density is (in atomic units)

$$\frac{T}{V} = \frac{3}{10}(3\pi^2)^{2/3}n^{5/3}. \tag{1.3}$$

The third term represents exchange energy, using local density approximation (LDA). The full derivation can be found in [1]:

$$\frac{E_X}{V} = -\frac{3}{4\pi}\left(3\pi^2\right)^{1/3} n^{4/3}. \tag{1.4}$$

The fourth term in the Lagrangian density corresponds to the Hartree potential, the electrostatic potential from electron charge density. In our case, the ion-ion interactions are included in the uniform charge background (jellium approximation). In an infinite solid matter, the electron-electron interactions and electron-ion interactions cancel each other out, therefore we obtain $V_h = 0$. However, in a finite particle, due to the spillout effect of electrons, the Hartree potential is nonzero. The Hartree potential satisfies the following Poisson equation (n_i denotes the ion density) [3]:

$$\Delta V_h = 4\pi(n - n_i).$$

The corresponding term in the Lagrangian density is

$$-\frac{\left(\nabla V_h\right)^2}{8\pi} + \left(n_i - n\right)V_h. \tag{1.5}$$

Finally, by combining all of the aforementioned terms, we obtain the Lagrangian density:

$$\begin{aligned}\mathscr{L} = n\left(\frac{\partial S}{\partial t} + \frac{(\nabla S)^2}{2}\right) + \frac{3}{10}\left(3\pi^2\right)^{2/3} n^{5/3} \\ - \frac{3}{4\pi}\left(3\pi^2\right)^{1/3} n^{4/3} - \frac{(\nabla V_h)^2}{8\pi} + (n_i - n)\, V_h.\end{aligned} \tag{1.6}$$

1.2 Derivation of QHD equations

We are now able to derive the Euler-Lagrange equations from the Lagrangian density in the following form

$$\sum_{\nu=0}^{3} \frac{\partial}{\partial x^\nu}\left(\frac{\partial \mathscr{L}}{\partial q_{a,\nu}}\right) - \frac{\partial \mathscr{L}}{\partial q_a} = 0,$$
$$\mathscr{L} = \mathscr{L}\left(q_a, q_{a,\nu}, x^\nu\right),$$

where x^ν is a space-time four-vector, q_a are functions which represent scalar fields (in our case, the fields are $n(\mathbf{r},t), S(\mathbf{r},t), V_h(\mathbf{r},t)$) and $q_{a,\nu}$ denotes a partial derivative $\frac{\partial q_a}{\partial x^\nu}$ [5]. Thus, we yield three equations:

$$\begin{aligned}\frac{\partial \mathscr{L}}{\partial n} &= \sum_{i=1}^{3} \frac{\partial}{\partial x_i}\left(\frac{\partial \mathscr{L}}{\partial \frac{\partial n}{\partial x_i}}\right) + \frac{\partial}{\partial t}\left(\frac{\partial \mathscr{L}}{\partial \frac{\partial n}{\partial t}}\right) \\ \frac{\partial \mathscr{L}}{\partial S} &= \sum_{i=1}^{3} \frac{\partial}{\partial x_i}\left(\frac{\partial \mathscr{L}}{\partial \frac{\partial S}{\partial x_i}}\right) + \frac{\partial}{\partial t}\left(\frac{\partial \mathscr{L}}{\partial \frac{\partial S}{\partial t}}\right) \\ \frac{\partial \mathscr{L}}{\partial V_h} &= \sum_{i=1}^{3} \frac{\partial}{\partial x_i}\left(\frac{\partial \mathscr{L}}{\partial \frac{\partial V_h}{\partial x_i}}\right) + \frac{\partial}{\partial t}\left(\frac{\partial \mathscr{L}}{\partial \frac{\partial V_h}{\partial t}}\right).\end{aligned}$$

By substituting $\mathscr{L}$ with the expression (1.6), we obtain motion equation, continuity equation and Poisson equation, respectively:

$$\frac{\partial \mathbf{u}}{\partial t} + \mathbf{u}\cdot\nabla\mathbf{u} = \nabla V_h - \nabla V_x - \nabla V_t \tag{1.7}$$

$$\frac{\partial n}{\partial t} + \nabla\cdot(n\mathbf{u}) = 0 \tag{1.8}$$

$$\Delta V_h = 4\pi(n - n_i). \tag{1.9}$$

The factor 4π in the equation (1.9) is due to the fact that we are using atomic units, where $\frac{1}{4\pi\epsilon_0} = 1$. The equation (1.7) resembles Newton's second law $\frac{d\mathbf{p}}{dt} = \mathbf{F}$, the expression on the left side corresponds to time derivative of momentum of electrons as a continuum, and the expression on the right side contains gradients of potentials,

which are equivalent to forces acting on the electrons. V_t and V_x signify potentials of kinetic energy and exchange interaction:

$$V_t = \frac{1}{2}(3\pi^2)^{2/3} n^{2/3},$$

$$V_x = -\frac{1}{\pi}(3\pi^2)^{1/3} n^{1/3}.$$

The potentials V_x, V_t are related to terms in the Lagrangian density in the following way (these expressions emerge upon applying the Euler-Lagrange method):

$$V_t = \frac{\partial}{\partial n}\left(\frac{T}{V}\right), \quad V_x = \frac{\partial}{\partial n}\left(\frac{E_x}{V}\right).$$

The Lagrangian density and QHD equations derived in this chapter are equivalent, as we can convert back and forth between the two. The QHD equations are nonlinear differential equations with three scalar fields $n(\mathbf{r}, t), S(\mathbf{r}, t), V_h(\mathbf{r}, t)$. In order to solve these equations, one could apply the finite element method [6]. However, we are going to take the approach of using an expected solution (ansatz) for electron density, which will allow us to gain a better insight into our system.

Chapter 2

Calculating the Lagrangian

2.1 Ansatz of the electron density

Our goal is to derive a set of differential equations dependent on two dynamic variables. To achieve this, we first need to determine an ansatz for the electron density and then determine the Lagrangian by integrating the Lagrangian density over space.

The chosen ansatz for the electron density [3, 4] is

$$n(\mathbf{r},t) = \frac{A}{1+\exp\left(\left(\frac{s(\mathbf{r},t)}{\sigma(t)}\right)^3 - \left(\frac{R}{\sigma_0}\right)^3\right)}, \tag{2.1}$$

where $\sigma(t)$ is the radial spillout of the electrons at the surface of the nanoparticle, σ_0 represents the spillout of the ground state and s is the displaced radial coordinate, $s(\mathbf{r},t) = \sqrt{x^2+y^2+(z-d(t))^2}$, where $\mathbf{r} = (x,y,z)^T$ and $d(t)$ is the displacement of center of mass of the electrons relative to fixed ion background, along the z-axis. By using this ansatz, we have parametrized the scalar field $n(\mathbf{r},t)$ with two time-dependent functions $\sigma(t)$ and $d(t)$, which are going to be our dynamic variables.

The normalization constant A is determined from the condition of integrating electron density over space $\int n d\mathbf{r} = N$:

$$A = \frac{3N}{4\pi\sigma^3}\frac{1}{\ln\left(1+\frac{1}{a}\right)}, \tag{2.2}$$

where a is a dimensionless quantity:

$$a = \exp\left(-\frac{R^3}{{\sigma_0}^3}\right). \tag{2.3}$$

The power of 3 was chosen in the ansatz (2.1), so that the normalization condition $\int n d\mathbf{r} = N$ can be calculated analytically. It is reasonable to use an ansatz in this form, because the density profile of the ansatz corresponds to the expected density profile - inside the nanoparticle ($r \leq R$), the density is equal to a constant, then

it smoothly decreases near the surface ($r = R$). The figure 2.1 shows the density profile given by ansatz at the ground state $\sigma = \sigma_0$ for three different values of $\frac{\sigma_0}{R}$.

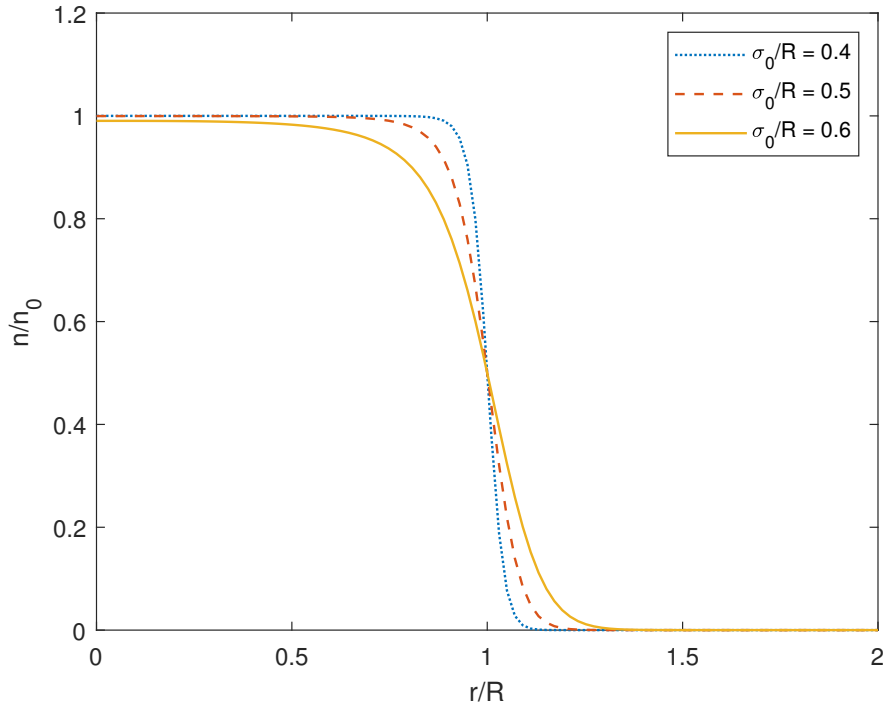

Figure 2.1: Electron density profile for three different values of $\frac{\sigma_0}{R}$

2.2 Expressing scalar fields as functions of dynamic variables

To begin with, we are going to express the two scalar fields $V_h(\mathbf{r}, t)$ and $S(\mathbf{r}, t)$ as functions of dynamic variables $\sigma(t)$ and $d(t)$ [3, 4]. Let's start with the field $S(\mathbf{r}, t)$. After inserting our ansatz (2.1) into the continuity equation (1.8), we obtain the velocity vector $\mathbf{u}(\mathbf{r}, t) = \nabla S$ (where $\mathbf{r} = (x, y, z)^T$):

$$\mathbf{u} = \left(\frac{\dot{\sigma}}{\sigma} x, \frac{\dot{\sigma}}{\sigma} y, \frac{\dot{\sigma}}{\sigma}(z - d) + \dot{d} \right)^T, \tag{2.4}$$

where dot signifies differentiation with respect to time, and subsequently

$$S = \frac{\dot{\sigma}}{2\sigma} s^2 + \dot{d}(z - d). \tag{2.5}$$

For the evaluation of Hartree potential $V_h(\mathbf{r}, t)$, we are going to modify the terms that correspond to the Hartee potential in the Lagrangian density (1.6), as this will prove to be useful during integration:

$$-\frac{(\nabla V_h)^2}{8\pi} + (n_i - n)V_h = -\frac{(\nabla V_h)^2}{8\pi} - \frac{V_h \Delta V_h}{4\pi} = \frac{(\nabla V_h)^2}{8\pi} - \frac{\nabla \cdot (V_h \nabla V_h)}{4\pi}. \tag{2.6}$$

After the first equal sign, we used the Poisson equation (1.9) and after the second one, identity $\nabla.(V_h \nabla V_h) = (\nabla V_h)^2 + V_h \Delta V_h$ was used. Next, we express the Hartee potential as separated contributions from electrons and ions: $V_h = V_e + V_i$. The individual potentials satisfy Poisson equations:

$$\Delta V_e = 4\pi n, \quad \Delta V_i = -4\pi n_i.$$

The ion potential V_i has spherical symmetry, therefore only radial part of the gradient of potential does not vanish. We integrate once over space in the radial coordinate and obtain

$$\frac{\partial V_i(r)}{\partial r} = \begin{cases} -\dfrac{N}{R^3} r \ , & r \leq R \\ -\dfrac{N}{r^2} \ , & r > R. \end{cases} \tag{2.7}$$

The term $\frac{\partial V_i}{\partial r}$ represents a force acting on one electron as a result of all the ions. In figure 2.2, this term is plotted as a function of r, for $R = 1\,\mathrm{nm}$:

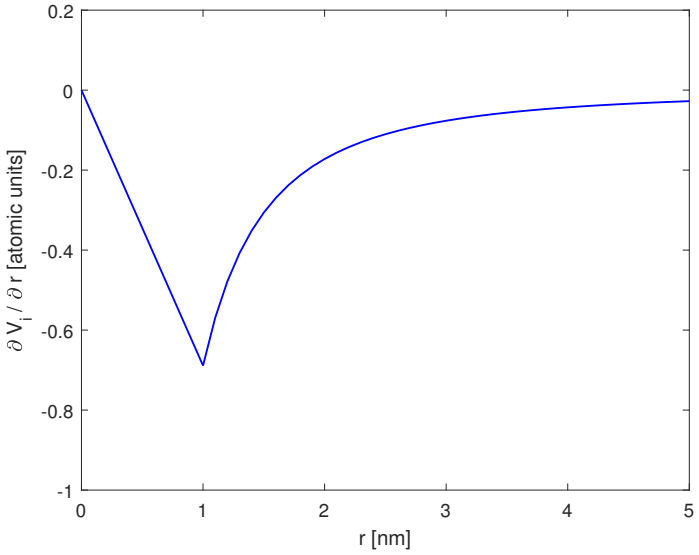

Figure 2.2: Plot of $\frac{\partial V_i}{\partial r}$ as a function of r, for $R = 1\,\mathrm{nm}$.

For the electron potential, we make use of an identity $\Delta = \frac{1}{r^2}\frac{\partial}{\partial r}\left(r^2 \frac{\partial}{\partial r}\right)$, as we have spherical symmetry. By combining this identity with the Poisson equation for electrons and integrating in the radial coordinate, we obtain the following expression:

$$s^2 \frac{\partial V_e(s,t)}{\partial s} = \frac{N}{\ln(1+\frac{1}{a})} \left(\frac{s^3}{\sigma^3} - \ln\left(1 + a \exp\left[\frac{s^3}{\sigma^3}\right]\right) + \ln(1+a) \right). \tag{2.8}$$

We can also rewrite this as a simpler expression (which, later on, we also found to be more numerically stable):

$$s^2 \frac{\partial V_e(s,t)}{\partial s} = \frac{N}{\ln(1+\frac{1}{a})} \ln\left(\frac{1+a}{a+\exp\left[-\frac{s^3}{\sigma^3}\right]}\right).$$

The term $\frac{\partial V_e}{\partial s}$ represents the force acting on one electron as a result of all the other electrons. In figure 2.3, this term is plotted as a function of s, for $R = 1\,\text{nm}$, for different values of $\sigma = \sigma_0$:

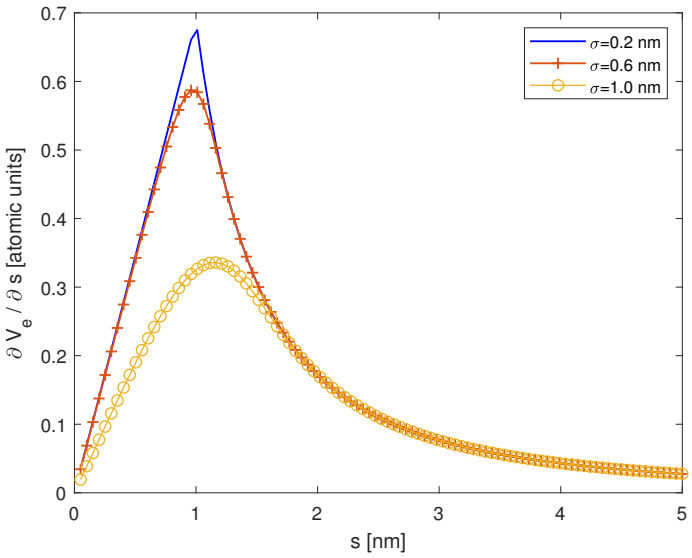

Figure 2.3: Plot of $\frac{\partial V_e}{\partial s}$ as a function of s, for $R = 1\,\text{nm}$, for different values of $\sigma = \sigma_0$.

Note that the ion potential is a function of the radial coordinate r, while the electron potential is a function of the displaced radial coordinate $s(t)$. This corresponds to the notion that the ions are fixed, while the center of mass of the electrons is free to move in such a way, that some electrons may get past the particle borders.

As we can see from the graphs, when the value of σ approaches zero, the plot of $\frac{\partial V_e}{\partial s}$ smoothly turns to $\frac{\partial V_i}{\partial r}$. This corresponds to the spillout effect getting smaller. For $\sigma = 0$ and $d = 0$, both the ions and electrons form a homogenous sphere of charge with its centre placed in the origin.

We have derived equations (2.1), (2.5), (2.7) and (2.8) for n, S, ∇V_h and thus expressed them as functions of our chosen dynamic variables. What's left to do is to determine $\frac{\partial S}{\partial t}$, $(\nabla S)^2$, $(\nabla n)^2$ as functions of the dynamic variables, as these expressions appear in the Lagrangian density, too. This task is straightforward and results directly from (2.1) and (2.5):

$$\frac{\partial S}{\partial t} = \frac{\ddot{\sigma}\sigma - \dot{\sigma}^2}{2\sigma^2} s^2 - \frac{\dot{\sigma}}{\sigma}\dot{d}\,(z-d) + \ddot{d}\,(z-d) - \dot{d}^2, \tag{2.9}$$

$$(\nabla S)^2 = \left(\frac{\dot{\sigma}}{\sigma}\right)^2 s^2 + 2\frac{\dot{\sigma}}{\sigma}\,(z-d)\,\dot{d} + \dot{d}^2, \tag{2.10}$$

$$(\nabla n)^2 = \frac{9a^2 s^4}{A^2\sigma^6} \exp\left(\frac{2s^3}{\sigma^3}\right) n^4. \tag{2.11}$$

2.3 Integrating the Lagrangian density over space

Now we are able to integrate the Lagrangian density over space and thereby obtain the Lagrangian $L = L(d, \sigma, \dot{d}, \dot{\sigma})$ [3, 4]:

$$\begin{aligned} L &= \int \mathscr{L} d\mathbf{r} \\ &= \underbrace{\int n\frac{\partial S}{\partial t} d\mathbf{r}}_{A} + \underbrace{\frac{1}{2}\int n\,(\nabla S)^2\, d\mathbf{r}}_{B} + \underbrace{\frac{3}{10}\left(3\pi^2\right)^{2/3}\int n^{5/3} d\mathbf{r}}_{C} \\ &\quad \underbrace{- \frac{3}{4\pi}\left(3\pi^2\right)^{1/3}\int n^{4/3} d\mathbf{r}}_{D} + \underbrace{\frac{1}{8\pi}\int (\nabla V_H)^2 d\mathbf{r}}_{E} \\ &\quad \underbrace{- \frac{1}{4\pi}\int \nabla\cdot(V_H \nabla V_H) d\mathbf{r}}_{F}. \end{aligned} \tag{2.12}$$

The term F is equal to zero, because it can be rewritten as a surface term using Gauss' divergence theorem, and we assume that the Hartree potential vanishes at infinity:

$$\int_V \nabla\cdot\mathbf{a}\; dV = \int_{\partial V} \mathbf{a}\cdot\mathbf{dS}, \quad \mathbf{a} = V_h \nabla V_h.$$

We are going to determine each remaining term individually:

- **Term A**:

$$\int n\frac{\partial S}{\partial t} d\mathbf{r} = \left(\frac{\ddot{\sigma}}{2\sigma} - \frac{\dot{\sigma}^2}{2\sigma^2}\right)\int n s^2 d\mathbf{r} + \left(\ddot{d} - \frac{\dot{\sigma}}{\sigma}\dot{d}\right)\int n\,(z-d)\, d\mathbf{r} - \dot{d}^2 \int n d\mathbf{r}$$

The second integral is equal to zero, because the function in the integral is odd. The third integral is easy to evalute too, as the integral corresponds to normalization condition and is equal to N. The first integral is more tricky:

$$\int ns^2 d\mathbf{r} = A \int \frac{s^2}{1 + a \exp\left(\frac{s^3}{\sigma^3}\right)} d\mathbf{s} = 4\pi A \int_0^\infty \frac{s^4}{1 + a \exp\left(\frac{s^3}{\sigma^3}\right)} ds = N\sigma^2 M(a),$$

where

$$M(a) = -\frac{\Gamma(\frac{5}{3})\mathrm{Li}_{5/3}(-\frac{1}{a})}{\ln(1 + \frac{1}{a})},$$

and Li is a polylogarithm function [3] (substitution $X = \frac{s}{\sigma}$ was used)

$$\mathrm{Li}_p(-\frac{1}{a}) = -\frac{1}{\Gamma(p)} \int_0^\infty \frac{X^{p-1}}{1 + a \exp(X)} dX,$$

where $\mathrm{Re}(p) > 0$, $\mathrm{Im}(a) = 0$, and $\frac{1}{a} > -1$.

Therefore:

$$\begin{aligned} \int n \frac{\partial S}{\partial t} d\mathbf{r} &= \frac{N}{2} M(a) \left(\ddot{\sigma}\sigma - \dot{\sigma}^2\right) - N\dot{d}^2 \\ &= \frac{N}{2} M(a) \left(\frac{d}{dt}\left(\sigma\dot{\sigma}\right) - 2\dot{\sigma}^2\right) - N\dot{d}^2 \\ &= -NM(a)\dot{\sigma}^2 - N\dot{d}^2, \end{aligned} \tag{2.13}$$

where we used the fact that the total time derivative $\frac{d}{dt}(\sigma\dot{\sigma})$ doesn't modify equations of motion and therefore can be crossed off.

- **Term B**:

$$\begin{aligned} \frac{1}{2} \int n \left(\nabla S\right)^2 d\mathbf{r} &= \frac{1}{2} \left(\frac{\dot{\sigma}}{\sigma}\right)^2 \int ns^2 d\mathbf{r} + \frac{\dot{\sigma}}{\sigma} \dot{d} \int (z - d)\, n d\mathbf{r} + \frac{\dot{d}^2}{2} \int n d\mathbf{r} \\ &= \frac{N}{2} M(a) \dot{\sigma}^2 + \frac{N}{2} \dot{d}^2 \end{aligned} \tag{2.14}$$

Integrals in term B can be computed analogically to integrals in term A.

- **Term C**:

$$\frac{3}{10} \left(3\pi^2\right)^{2/3} \int n^{5/3} d\mathbf{r} = \frac{N^{5/3}}{\sigma^2} f_F(a), \tag{2.15}$$

where $f_F(a)$ is (substitution $X = \frac{s}{\sigma}$ was used)

$$f_F(a) = \frac{6}{5}(3\pi)^{2/3}\left(\frac{3}{4\ln(1+\frac{1}{a})}\right)^{5/3}\int_0^\infty \frac{X^2}{(1+a\exp(X^3))^{5/3}}dX.$$

The integral appearing in the expression of f_F cannot be solved analytically and therefore cannot be further simplified. However, it can be computed numerically once we choose a specific value of a, which will be dealt with in the next chapter.

- **Term D**:

$$\frac{3}{4\pi}\left(3\pi^2\right)^{1/3}\int n^{4/3}d\mathbf{r} = \frac{N^{4/3}}{\sigma}f_X(a), \tag{2.16}$$

where f_X is (substitution $X = \frac{s}{\sigma}$ was used)

$$f_X(a) = \left(\frac{9}{4\sqrt{\pi}\ln(1+\frac{1}{a})}\right)^{4/3}\int_0^\infty \frac{X^2}{(1+a\exp(X^3))^{4/3}}dX.$$

- **Term E**:

The last term corresponding to the Hartree potential is the most complicated to evaluate. Firstly, we separate V_h into its constituent parts as we did before, $V_h = V_e + V_i$:

$$\frac{1}{8\pi}\int(\nabla V_h)^2 d\mathbf{r} = \frac{1}{8\pi}\left(\int(\nabla V_i)^2 d\mathbf{r} + \int(\nabla V_e)^2 d\mathbf{r} + 2\int \nabla V_i\cdot\nabla V_e d\mathbf{r}\right).$$

The first integral doesn't depend on dynamic variables, therefore won't modify equations of motions and can be crossed off. Let us evaluate the second integral, using the expression (2.8) and substitution $X = \frac{s}{\sigma}$:

$$\begin{aligned}
\int(\nabla V_e)^2 d\mathbf{r} &= \int\left(\frac{\partial V_e}{\partial s}\right)^2 d\mathbf{r} \\
&= \int \frac{N^2}{(\ln(1+\frac{1}{a}))^2}\frac{1}{s^4}\left(\frac{s^3}{\sigma^3} - \ln\left(1+a\exp\left[\frac{s^3}{\sigma^3}\right]\right) + \ln(1+a)\right)^2 d\mathbf{s} \\
&= \frac{4\pi N^2}{(\ln(1+\frac{1}{a}))^2}\int_0^\infty \frac{1}{s^2}\left(\frac{s^3}{\sigma^3} - \ln\left(1+a\exp\left[\frac{s^3}{\sigma^3}\right]\right) + \ln(1+a)\right)^2 ds \\
&= \frac{8\pi N^2}{\sigma}f_{ee}(a),
\end{aligned} \tag{2.17}$$

where $f_{ee}(a)$ is

$$f_{ee}(a) = \frac{1}{2\left(\ln(1+\frac{1}{a})\right)^2}\int_0^\infty \frac{1}{X^2}\left(X^3 + \ln(1+a) - \ln\left[1 + a\exp(X^3)\right]\right)^2 dX.$$

Now, let us evaluate the third integral:

$$\begin{aligned} I \equiv \int \nabla V_e \cdot \nabla V_i &= \int \frac{\partial V_i}{\partial r}\frac{\partial V_e}{\partial s}\frac{1}{sr}(r^2 - zd)d\mathbf{r} \\ &= \frac{2\pi N}{\ln(1+\frac{1}{a})}\int \frac{\partial V_i}{\partial r}\frac{r^2\sin\theta}{s^3}\left(r - d\cos\theta\right) \\ &\times \left(\frac{s^3}{\sigma^3} - \ln\left(1 + a\exp\left[\frac{s^3}{\sigma^3}\right]\right) + \ln(1+a)\right) dr d\theta. \end{aligned}$$

Here we used a substitution $z = rcos\theta$. This integral, however, does not have spherical symmetry, which is why we need to use a different approach. To proceed, we develop the displaced radial coordinate $s = \sqrt{x^2 + y^2 + (z-d)^2}$ as a power series of d [4]:

$$s = r - d\cos\theta + d^2\frac{\sin^2\theta}{2r} + d^3\frac{cos\theta - cos^3\theta}{2r^2} - d^4\frac{1 - 6cos^2\theta + 5cos^4\theta}{8r^3} + O(d^5).$$

After we substitute s in the integral, we obtain the following expression:

$$I = -\frac{4\pi N^2}{R}f_{ei}(\sigma) + 2\pi N\Omega_d^2(\sigma)d^2 - 4\pi N K(\sigma)d^4 + \cdots . \tag{2.18}$$

As we can see, the odd power doesn't appear in the final expression, because of the symmetry in the (x, y) plane, as d and $-d$ are equivalent. $f_{ei}(\sigma)$, $\Omega_d^2(\sigma)$ and $K(\sigma)$ are defined as

$$\begin{aligned} f_{ei}(\sigma) &= \frac{1}{\ln(1+\frac{1}{a})}\left(\frac{\sigma^2}{R^2}\int_0^{R/\sigma} X\Big[X^3 + \ln(1+a)\right. \\ &\left. - \ln\left(1 + a\exp\left(X^3\right)\right)\Big]dX + \frac{R}{\sigma}\int_{R/\sigma}^\infty \frac{dX}{X^2}\Big[X^3\right. \\ &\left. + \ln(1+a) - \ln\left(1 + a\exp\left(X^3\right)\right)\Big]\right), \\ \Omega_d^2(\sigma) &= \frac{N}{R^3\ln(1+\frac{1}{a})}\left(\frac{R^3}{\sigma^3} + \ln\left(1 + \frac{1}{a}\right)\right. \\ &\left. - \ln\left[1 + a\exp\left(\frac{R^3}{\sigma^3}\right)\right]\right), \\ K(\sigma) &= \frac{9NRa}{40\ln(1+\frac{1}{a})\sigma^6}\,\frac{\exp\left(\frac{R^3}{\sigma^3}\right)}{\left(1 + a\exp\left(\frac{R^3}{\sigma^3}\right)\right)^2}. \end{aligned}$$

2.4 Evaluating the Lagrangian

In order to obtain the final form of the Lagrangian, we are going to combine expressions (2.13), (2.14), (2.15), (2.16), (2.17) and (2.18):

$$L = -\frac{1}{2}NM(a)\dot{\sigma}^2 - \frac{1}{2}N\dot{d}^2 + \frac{N{\Omega_d}^2(\sigma)d^2}{2} - NK(\sigma)d^4 + \frac{N^{5/3}}{\sigma^2}f_F(a) - \frac{N^{4/3}}{\sigma}f_x(a) + \frac{N^2}{\sigma}f_{ee}(a) - \frac{N^2}{R^2}f_{ei}(\sigma).$$

For convenience purposes, we are going to multiply the obtained Lagrangian with a factor of $-\frac{1}{N}$ and introduce a pseudopotential $U(\sigma)$ [4]:

$$L = \frac{1}{2}M(a)\dot{\sigma}^2 + \frac{1}{2}\dot{d}^2 - \frac{{\Omega_d}^2(\sigma)d^2}{2} + K(\sigma)d^4 - U(\sigma), \tag{2.19}$$

$$U(\sigma) = \frac{N^{2/3}}{\sigma^2}f_F(a) - \frac{N^{1/3}}{\sigma}f_x(a) + \frac{N}{\sigma}f_{ee}(a) - \frac{N}{R}f_{ei}(\sigma). \tag{2.20}$$

Note that the first two terms in the Lagrangian correspond to kinetic energy, where $M(a)$ is an effective mass of the breathing mode. The third and fourth term in the Lagrangian represent second and fourth order of electron-ion interacting energy. The last term pseudopotential $U(\sigma)$ determines the ground state, as will be discussed in the next chapter.

2.5 Deriving equations of motion

Now that we have obtained the Lagrangian, we can use the Euler-Lagrange method [5] and derive equations of motion dependent on two dynamic variables σ and d:

$$\ddot{d} = -{\Omega_d}^2(\sigma)d + 4K(\sigma)d^3, \tag{2.21}$$

$$\ddot{\sigma} = \frac{1}{M(a)}\left[-\frac{dU(\sigma)}{d\sigma} - \Omega_d(\sigma)\frac{d\Omega_d(\sigma)}{d\sigma}d^2 + \frac{dK(\sigma)}{d\sigma}d^4 \right]. \tag{2.22}$$

The second equation can be expressed analytically in the following way:

$$\ddot{\sigma} = \frac{1}{M(a)}\left[-\frac{dU(\sigma)}{d\sigma} + \frac{3Nd^2}{2\sigma^4\ln(1+\frac{1}{a})}\frac{1}{1+a\exp(\frac{R^3}{\sigma^3})} - \frac{27NRa\exp(\frac{R^3}{\sigma^3})d^4}{40\ln(1+\frac{1}{a})\sigma^{10}}\frac{\left(1-a\exp(\frac{R^3}{\sigma^3})\right)R^3 + 2\left(1+a\exp(\frac{R^3}{\sigma^3})\right)\sigma^3}{\left(1+a\exp(\frac{R^3}{\sigma^3})\right)^3} \right]. \tag{2.23}$$

This is a crucial result, as we have transformed the complicated problem of electron dynamics into a set of two coupled differential equations. In the next chapter, we are going to determine the ground state and analyze the terms in the obtained Lagrangian.

Chapter 3

The ground state

3.1 Determining the ground state

In this chapter, we will determine the ground state, for which $\sigma = \sigma_0$ and $d = 0$. We can obtain the condition for ground state by setting time derivatives of σ and d in (2.21) and (2.22) equal to zero. The first equation will be satisfied automatically and the second equation gives us the condition for the ground state:

$$\frac{dU(\sigma)}{d\sigma} = 0.$$

Thus, we want to find the value $\sigma = \sigma_0$, for which the pseudopotential $U(\sigma = \sigma_0)$ is minimal. The pseudopotential was derived in the previous chapter:

$$U(\sigma) = \frac{N^{2/3}}{\sigma^2} f_F(a) - \frac{N^{1/3}}{\sigma} f_x(a) + \frac{N}{\sigma} f_{ee}(a) - \frac{N}{R} f_{ei}(\sigma). \tag{3.1}$$

We will find the ground state by substituting N, R and σ in the pseudopotential with specific values. Firstly, we need to determine the number of electrons N depending on the radius R of the particle. We are going to investigate values $R = 1, 1.5, 2\,\text{nm}$. Below $1\dot{\text{n}}\text{m}$, quantum effects become very significant, and above $2\,\text{nm}$, the ansatz may no longer hold [3]. The number of electrons N is given by

$$N = \frac{\frac{4}{3}\pi R^3}{V_{\text{atom}}} N_{e^-/\text{atom}}.$$

The nanoparticle is golden with FCC structure, therefore, the lattice constant is $a = 4.08$ Å$= 0.408\,\text{nm}$ [7], and so the volume of one atom can be expressed as

$$V_{\text{atom}} = \frac{a^3}{\text{number of atoms in basis}} = \frac{0.408^3}{4}.$$

We will investigate two possible alternatives:

1) $N_{e^-/\text{atom}} = 1$, thus, we get $N = 246,\ 832,\ 1971$ for $R = 1,\ 1.5,\ 2\,\text{nm}$, respectively.

2) $N_{e^-/\text{atom}} = 11$, in which case we will get $N = 246 * 11,\ 832 * 11,\ 1971 * 11$ for $R = 1,\ 1.5,\ 2\,\text{nm}$.

Both of these options are reasonable to use. The number 1 corresponds to $6s^1$ electron, which is the only electron forming the Fermi level. Number 11 consists of additional $5d^{10}$ valence electrons. It is unclear which option is better, therefore, we will use both and compare the obtained results.

The ground state $\sigma = \sigma_0$ can be determined in the following way: we graph the dependance of pseudopotential U on $\sigma = \sigma_0$ and the minimum of the function determines the spillout σ_0 of the ground state.

The following figures 3.1, 3.2, 3.3 show $U(\sigma = \sigma_0)$:

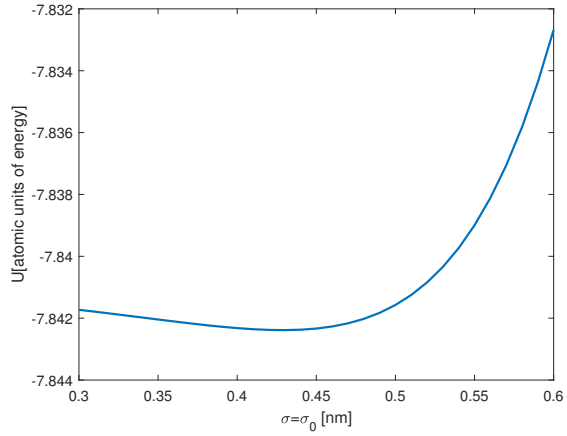

(a) $N_{e^-/\text{atom}} = 1$

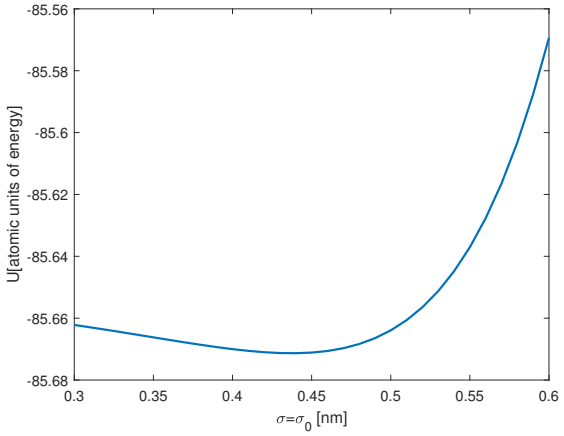

(b) $N_{e^-/\text{atom}} = 11$

Figure 3.1: $U(\sigma = \sigma_0)$ for $R = 1\,\text{nm}$

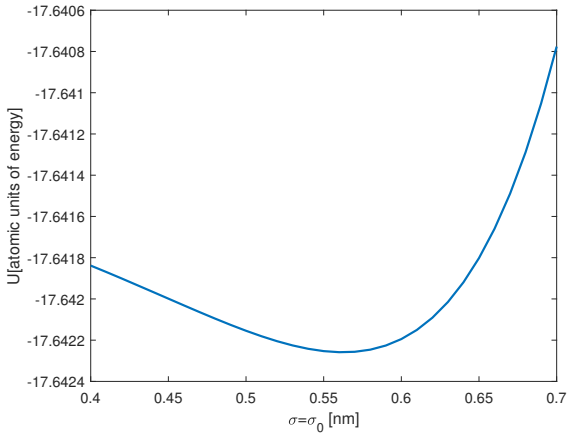

(a) $N_{e^-/\text{atom}} = 1$

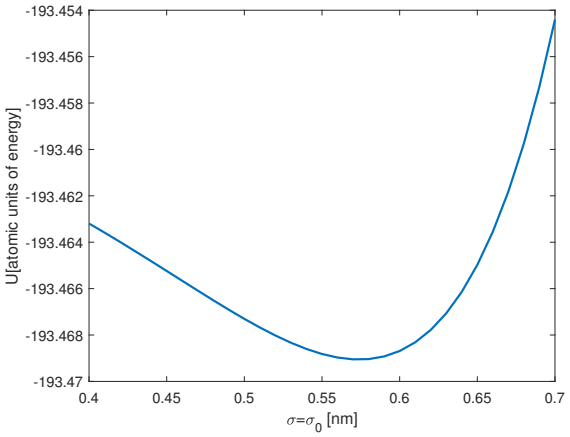

(b) $N_{e^-/\text{atom}} = 11$

Figure 3.2: $U(\sigma = \sigma_0)$ for $R = 1.5\,\text{nm}$

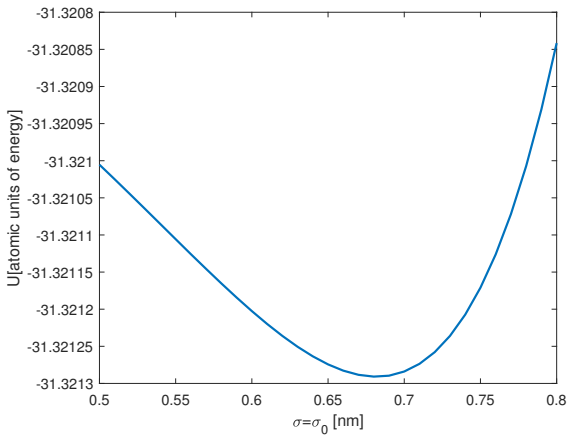

(a) $N_{e^-/\text{atom}} = 1$

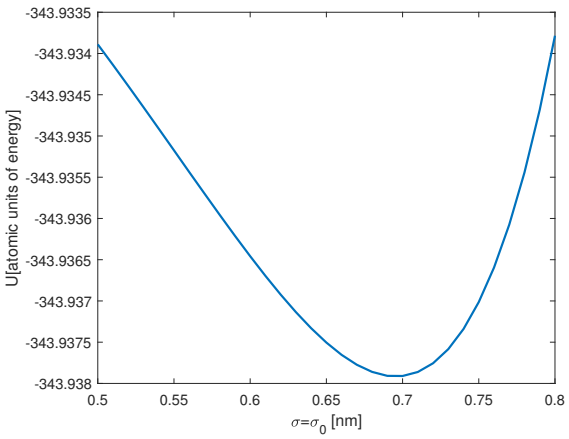

(b) $N_{e^-/\text{atom}} = 11$

Figure 3.3: $U(\sigma = \sigma_0)$ for $R = 2\,\text{nm}$

From these graphs, we can deduce the value of ground state σ_0 for each case. The results are summarized in the following table (note that the actual values used later on in this thesis are more precise, the results in the table are rounded to 2 decimal places):

R [nm]	σ_0 [nm] (1 e^-)	σ_0 [nm] (11 e^-)
1	0.43	0.44
1.5	0.56	0.57
2	0.68	0.70

Table 3.1: The values of spillout σ_0 at ground state depending on particle radius

As we can see, the choice of number of electrons per atom didn't impact the value of σ_0 much. We will use $N_{e^-/\text{atom}} = 1$ from now, which is also in agreement with publications [3, 4].

Now that we have obtained the value of the ground state σ_0, we are able to plot the pseudopotential $U(\sigma, \sigma_0)$ (note that σ and σ_0 are no longer identical, now we have inserted the obtained value of σ_0 into the pseudopotential - σ_0 appears in the pseudopotential in the constant $a = \exp(-R^3/{\sigma_0}^3)$ - and we are plotting U as a function of σ):

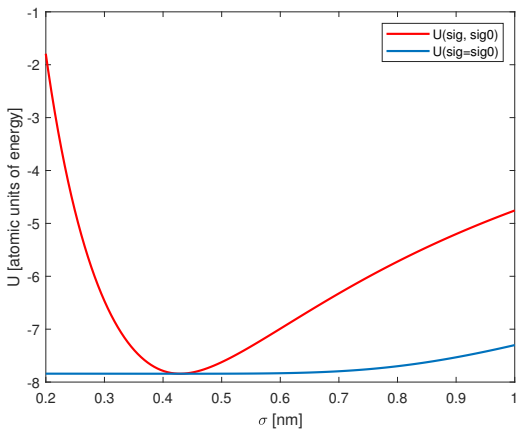

Figure 3.4: Pseudopotential U as a function of σ, with inserted obtained value of σ_0 (red) vs $U(\sigma = \sigma_0)$ which was used to determine the value of σ_0 (blue), for $R = 1\,\text{nm}$, $N = 246$

3.2 Analyzing terms in the pseudopotential $U(\sigma = \sigma_0)$

In the figure 3.6 and 3.5, we can see individual terms in the pseudopotential $U(\sigma = \sigma_0)$ and how they change depending on $\sigma = \sigma_0$. The Fermi pressure and exchange interaction don't change much relative to electron-electron interactions and electron-ion interactions. After summing up electron-electron interaction and electron-ion interaction into one collective Coulombic interaction term, we can see, that the contributions of individual terms in pseudopotential $U(\sigma = \sigma_0)$ become more intricate.

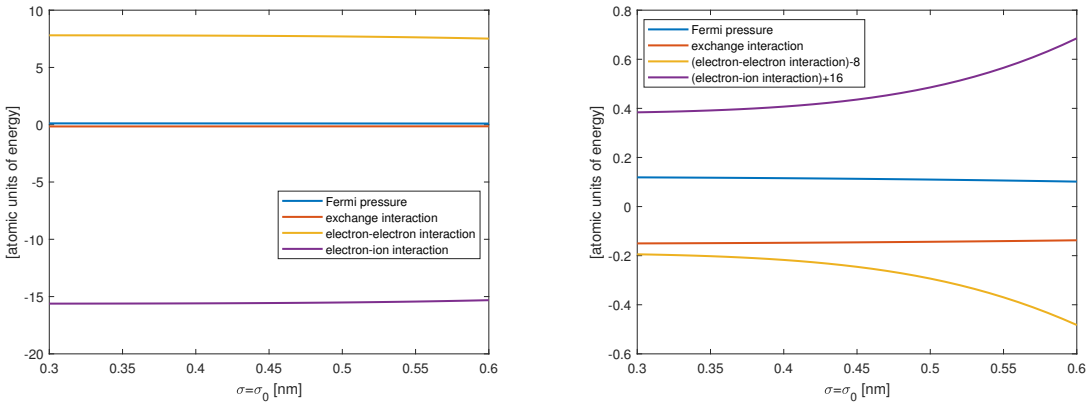

Figure 3.5: Dependance of terms in the pseudopotential $U(\sigma = \sigma_0)$ for $R = 1\,\text{nm}$, in the second graph, values were moved along y-axis for better clarity

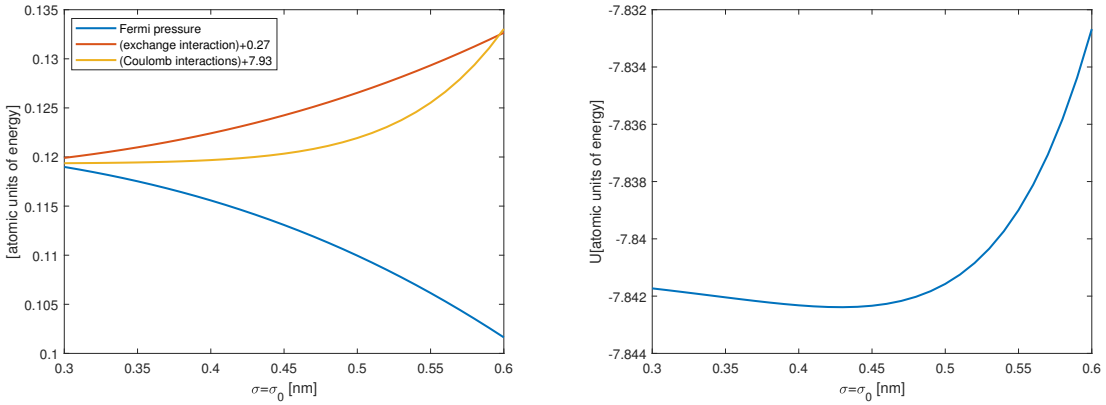

Figure 3.6: Dependance of terms in the pseudopotential $U(\sigma = \sigma_0)$, for $R = 1\,\mathrm{nm}$, in the first graph, values were moved along y-axis for better clarity, the second graph depicts all the terms of $U(\sigma = \sigma_0)$ summed up

3.3 Analyzing electron-ion interacting energy

Next, we are going to investigate the second and fourth order terms of electron-ion interacting energy in the Lagrangian (2.19) (note that we have already inserted the determined value σ_0 into these expressions and are studying dependance on σ):

$$E_{ei}(d) = \frac{{\Omega_d}^2(\sigma)d^2}{2} - K(\sigma)d^4 \tag{3.2}$$

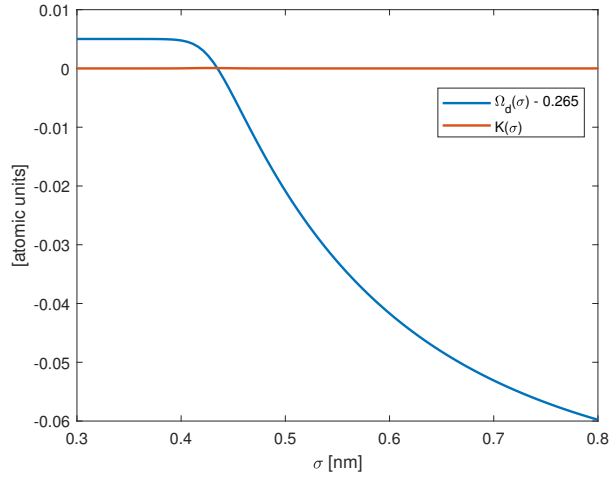

Figure 3.7: $\Omega_d(\sigma)$ and $K(\sigma)$ for $R = 1\,\mathrm{nm}$, the value of $\Omega_d(\sigma)$ was moved along the y-axis for better clarity

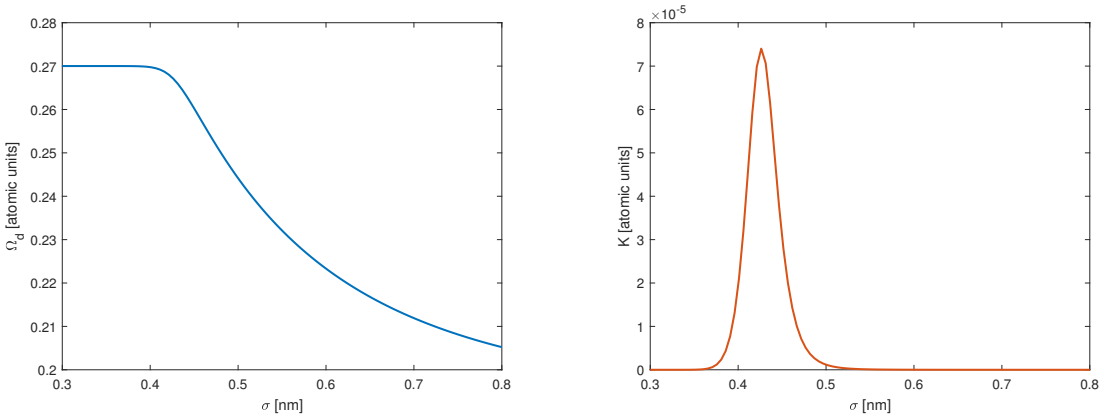

Figure 3.8: $\Omega_d(\sigma)$ and $K(\sigma)$ for $R = 1\,\mathrm{nm}$

As we can see from figures 3.7 and 3.8, $K(\sigma)$ changes only slightly relative to $\Omega_d(\sigma)$ as a function of σ. $\Omega_d(\sigma)$ remains constant up until the value $\sigma_0 = 0.43\,\mathrm{nm}$, then it gradually decreases. $K(\sigma)$ reaches its maximum at $\sigma_0 = 0.43\,\mathrm{nm}$.

Chapter 4

Determining eigenfrequencies of oscillations of $d(t)$ and $\sigma(t)$

4.1 Solving the equations of motion using the Runge-Kutta method

So far, we have been dealing with determining the ground state of our system. Now, we are going to determine the eigenfrequencies of oscillations of $d(t)$ and $\sigma(t)$ (no external electric field yet, zero damping) by solving the derived equations of motion:

$$\ddot{d} = -{\Omega_d}^2(\sigma)d + 4K(\sigma)d^3, \tag{4.1}$$

$$\ddot{\sigma} = \frac{1}{M(a)}\left[-\frac{dU(\sigma)}{d\sigma} - \Omega_d(\sigma)\frac{d\Omega_d(\sigma)}{d\sigma}d^2 + \frac{dK(\sigma)}{d\sigma}d^4 \right]. \tag{4.2}$$

In our system, we can observe two modes: oscillations of $\sigma(t)$ and oscillations of $d(t)$. These can also be referred to as the breathing mode and the dipole mode, respectively [3]. The oscillation of $d(t)$ represents electron density oscillations with respect to the fixed ion background along the z-axis. The oscillation of $\sigma(t)$ represents the radial flow of charge density of electrons outward from the center of nanoparticle (when the change of σ is positive) and inward (when the change of σ is negative).

Because $d(t)$ and $\sigma(t)$ appear in both equations, the two equations of motion are coupled. We will solve them numerically using Runge-Kutta method of order 4 [8]. In order to use this method, we are going to rewrite the equations (4.1), (4.2) as a system of first-order differential equations in the following way:

$$\dot{y}_1 = y_2 \tag{4.3}$$

$$\dot{y}_2 = -{\Omega_d}^2(y_3)y_1 + 4K(y_3){y_1}^3 \tag{4.4}$$

$$\dot{y}_3 = y_4 \tag{4.5}$$

$$\dot{y}_4 = \frac{1}{M(a)} \left(-\frac{dU(y_3)}{dy_3} - \Omega_d(y_3) \frac{d\Omega_d(y_3)}{dy_3} {y_1}^2 + \frac{dK(y_3)}{dy_3} {y_1}^4 \right) \tag{4.6}$$

In the equations, $y_1(t), y_2(t), y_3(t), y_4(t)$ represent $d(t), \dot{d}(t), \sigma(t), \dot{\sigma}(t)$, respectively. Additionally, we have to determine the initial conditions for our system of differential equations:

$$\begin{aligned} y_1(0) &\equiv d(0) = 0 \\ y_2(0) &\equiv \dot{d}(0) \\ y_3(0) &\equiv \sigma(0) = \sigma_0 \\ y_4(0) &\equiv \dot{\sigma}(0). \end{aligned}$$

The initial condition $d(0) = 0$ represents the initial displacement of the center of mass of electrons with respect to the center of the nanoparticle. The initial condition $\sigma(0) = \sigma_0$ represents the fact that our system is initially in the ground state. Our system will be excited by either $\dot{d}(0)$ or $\dot{\sigma}(0)$. These values will be varied and investigated later on.

Now, we can implement the Runge Kutta method for our system of first-order differential equations:

$$\begin{aligned} \dot{y}_i &= f_i(t, y) \\ y_i(0) &= y_{0i}, \end{aligned}$$

where $i = 1, 2, 3, 4$ and $y = (y_1, y_2, y_3, y_4)$. In the method of Runge Kutta, we start with our initial condition y_{0i} and consecutively calculate $y_i(t^k) = y_i^k$, where $t^k = t_0 + kh = kh$ and h is the step size:

$$\begin{aligned} y_i^{k+1} &= y_i^k + h/6 \left(K_i^1 + 2K_i^2 + 2K_i^3 + K_i^4 \right) \\ K_i^1 &= f_i(t^k, y^k) \\ K_i^2 &= f_i(t^k + h/2, y^k + hK^1/2) \\ K_i^3 &= f_i(t^k + h/2, y^k + hK^2/2) \\ K_i^4 &= f_i(t^k + h, y^k + hK^3). \end{aligned}$$

We can implement this method by using a loop cycle and calculate y_i^k for any time t^k, for $i = 1, 2, 3, 4$.

We implemented this method in Matlab with the following parameters:

$$\begin{aligned} R &= 1 \text{ nm} \approx 18.897 \text{ AU} \\ N &= 246 \\ \sigma_0 &= 0.4290 \text{ nm} \approx 8.107 \text{ AU} \\ h &= 0.1\text{AU} \\ t_{max} &= 48.38 \text{ fs} \approx 2000 \text{ AU} \end{aligned}$$

The value of σ_0 was calculated in the previous chapter. The maximum time was chosen in such a way as to depict sufficient number of oscillations (in the order of 10^1) .

In order to solve the equations, the derivative of pseudopotential $\frac{dU}{d\sigma}$ is needed. To remind ourselves, we expressed the pseudopotential in the following way:

$$U(\sigma) = \frac{N^{2/3}}{\sigma^2} f_F(a) - \frac{N^{1/3}}{\sigma} f_x(a) + \frac{N}{\sigma} f_{ee}(a) - \frac{N}{R} f_{ei}(\sigma).$$

Because the values R and σ_0 are fixed for our case, the terms $M(a), f_F(a)$, $f_x(a), f_{ee}(a)$ in pseudopotential $U(\sigma)$ are all constants, as a only depends on R and σ_0, and therefore is a constant, too. Thus, the first three terms of the pseudopotential are very easy to derivate and express analytically.

The fourth term is less straightforward, as the dependance on σ is quite complicated and the derivative cannot be expressed analytically. The first approach we tried was to derivate the expression $f_{ei}(\sigma)$ numerically, then fit the derivative with a polynomial and insert the polynomial expression into our equations of motion in the Runge Kutta method implementation. However, a method we found worked better and was numerically more stable, was to define the derivative of pseudopotential as a function of σ directly in the Runge Kutta implementation in the following way:

$$\frac{dU}{d\sigma}(\sigma) = \frac{U(\sigma + \Delta\sigma) - U(\sigma - \Delta\sigma)}{2\Delta\sigma},$$

where we chose $\Delta\sigma = 0.01$. We took the same approach with $\frac{d\Omega_d}{d\sigma}$ and $\frac{dK}{d\sigma}$:

$$\frac{d\Omega_d}{d\sigma}(\sigma) = \frac{\Omega_d(\sigma + \Delta\sigma) - \Omega_d(\sigma - \Delta\sigma)}{2\Delta\sigma},$$

$$\frac{dK}{d\sigma}(\sigma) = \frac{K(\sigma + \Delta\sigma) - K(\sigma - \Delta\sigma)}{2\Delta\sigma}.$$

After executing the Matlab code with various different values of initial derivatives $\dot{\sigma}(0)$ and $\dot{d}(0)$, we observed the following results:

- If both the initial derivatives are chosen to be $\dot{\sigma}(0) = 0$ and $\dot{d}(0) = 0$ (trivial case), then there are no oscillations of $\sigma(t)$ and $d(t)$ and their values are given by initial conditions $d(t) = 0$, $\sigma(t) = \sigma_0$
- If $\dot{\sigma}(0) = 0$ and $\dot{d}(0)$ is chosen to be nonzero, both $\sigma(t)$ and $d(t)$ oscillate

- If $\dot{d}(0) = 0$ and $\dot{\sigma}(0)$ is chosen to be nonzero, $\sigma(t)$ oscillates, however, $d(t)$ does not start to oscillate, even if we choose a large value $\dot{\sigma}(0)$. The coupling between the dynamical variables $d(t)$ and $\sigma(t)$ is such that oscillations of $d(t)$ are able to excite oscillations of $\sigma(t)$, but not the other way around.
- If we choose the initial derivatives to be too large, $\sigma(t)$ diverges (not shown). This could be interpreted as removing the electrons from the atom completely, which goes beyond applicability of our model.

4.2 Oscillations of $d(t)$ and $\sigma(t)$ for different initial conditions

1. Let us first have a look at the case of $\dot{\sigma}(0) = 0$ and $\dot{d}(0) \neq 0$:

   In the figures 4.1 and 4.2, we can see the oscillations of $d(t)$, for different values $\dot{d}(0) = 0.001,\ 0.005,\ 0.01,\ 0.05,\ 0.1,\ 0.5$. For increasing value of $\dot{d}(0)$, the amplitude of oscillations increases, while the frequency remains the same.

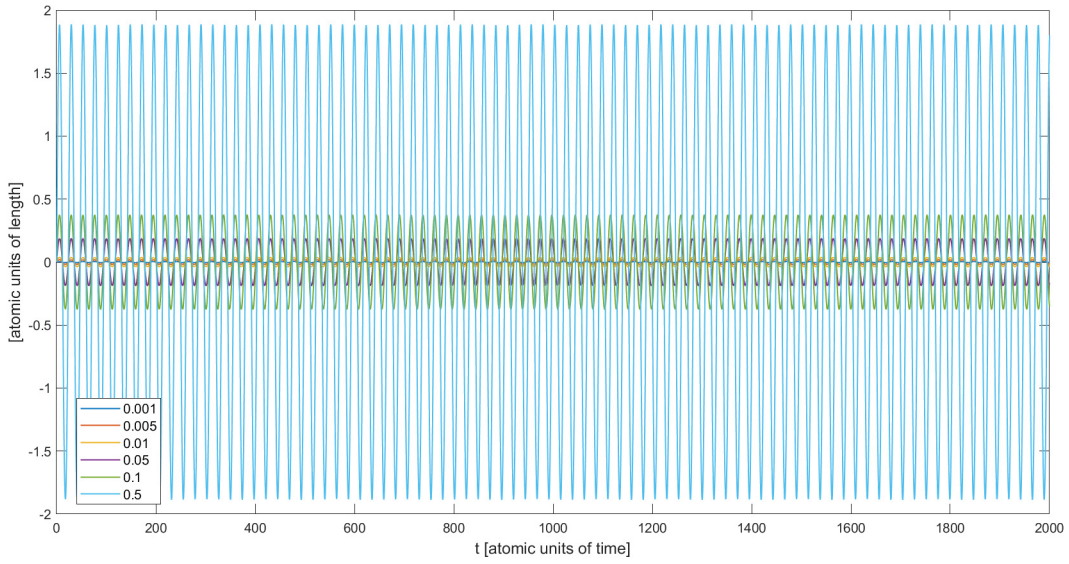

Figure 4.1: Amplitude of oscillations of $d(t)$ in atomic units for different values of $\dot{d}(0)$

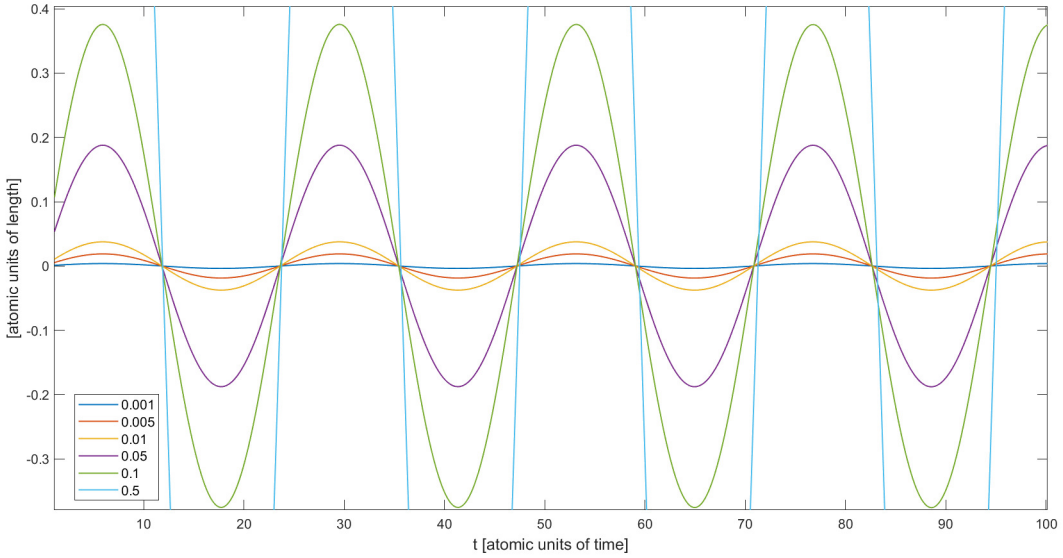

Figure 4.2: Amplitude of oscillations of $d(t)$ in atomic units for different values of $\dot{d}(0)$, zoomed in for better clarity

In the figures 4.3 and 4.4, we can see the oscillations of $\sigma(t)$, for different values $\dot{d}(0) = 0.001,\ 0.005,\ 0.01,\ 0.05,\ 0.1,\ 0.5$.

We can observe, that for smaller values $\dot{d}(0)$, the oscillations of $\sigma(t)$ are nearly identical. We can also notice, that the equilibrium value, around which $\sigma(t)$ oscillates, isn't σ_0, rather a slightly higher value. We will observe this exact same phenomenon in the next chapter as well. It is most likely due to the shape of the pseudopotential $U(\sigma, \sigma_0)$, visualized in figure 3.4 in red. The curvature of $U(\sigma, \sigma_0)$ is steeper on the left, causing the equilibrium value of the oscillations to steer towards higher values.

Furthermore, for values $\dot{d}(0)$ above 0.1, the behaviour of oscillations starts to become nonlinear. As it has already been mentioned, for values that are too large, (values in the order of 10^0) $\sigma(t)$ will diverge.

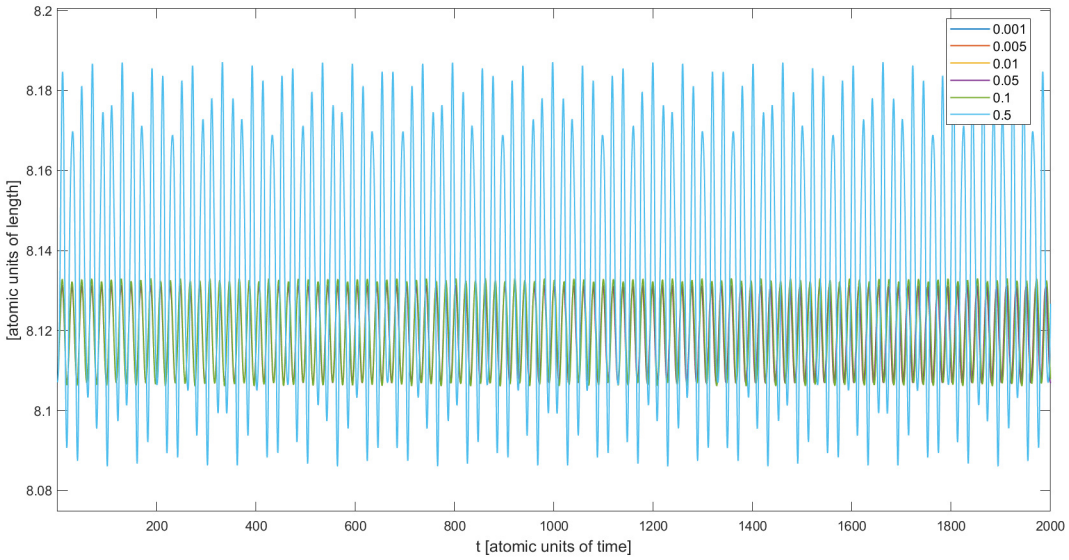

Figure 4.3: Amplitude of oscillations of $\sigma(t)$ in atomic units for different values of $\dot{d}(0)$

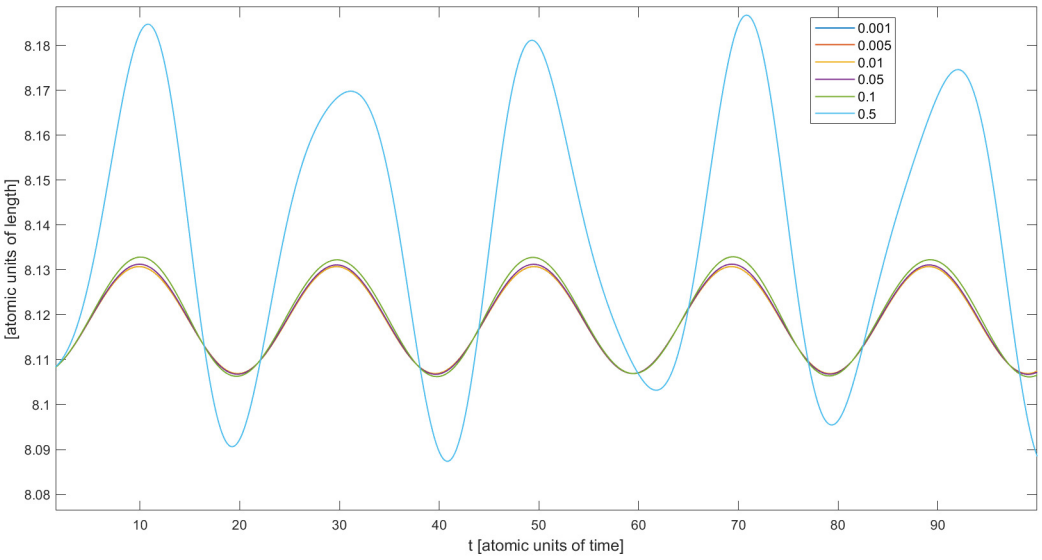

Figure 4.4: Amplitude of oscillations of $\sigma(t)$ in atomic units for different values of $\dot{d}(0)$, zoomed in for better clarity

Using the fast Fourier transform, we were able to visualize frequencies of oscillations of $d(t)$ and $\sigma(t)$ for different initial values of $\dot{d}(0)$, in figure 4.5. Color denotes amplitude of oscillations of $d(t)$ or $\sigma(t)$. It is worth noting that the only relevant output is the specific oscillation frequency, which is distinctly visible, the background and discontinuities in color for some specific initial values have no physical meaning. They are purely numerical artifacts, as they depend strongly on the size of the time step and/or the maximum time.

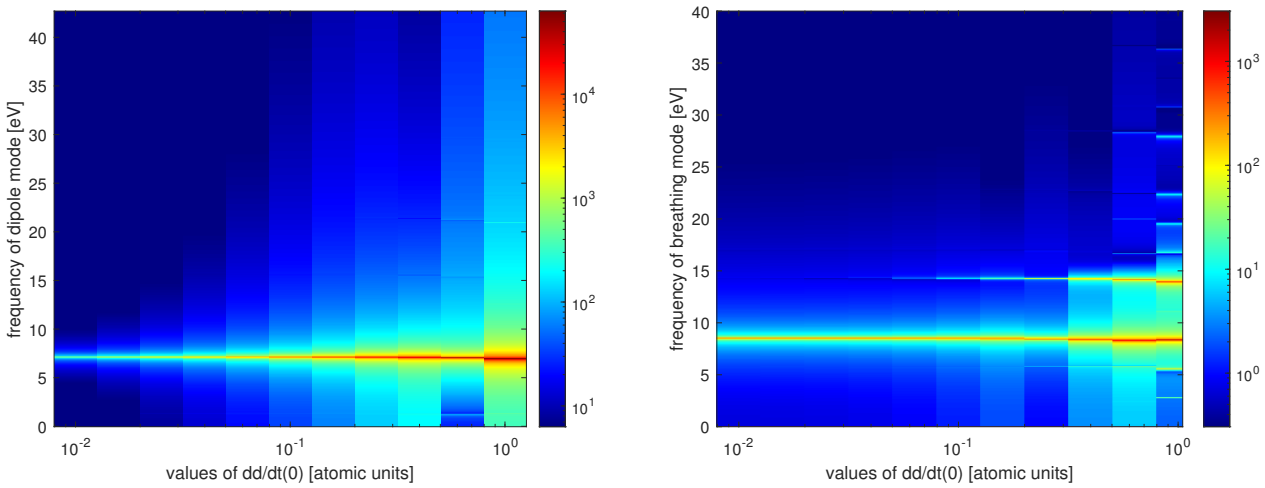

Figure 4.5: Frequency of oscillations of $d(t)$ (dipole mode) and $\sigma(t)$ (breathing mode) depending on different values of $\dot{d}(0)$

In the graph depicting frequency of dipole mode, there is a very strong resonant frequency, which corresponds to our model: $\Omega_d(\sigma_0) = 0.2663\,\text{AU}$ (corresponds to $7.246\,\text{eV}$). There are other frequencies appearing at larger values of initial conditions, but these are very faint compared to the resonant frequency and could just be numerical artifacts.

In the graph depicting frequency of the breathing mode, there is one main frequency at $8.3\,\text{eV}$ and another one appearing for larger values of initial conditions, which corresponds to $2\Omega_d(\sigma_0)$, as we are using $\dot{d}(0)$ to excite our system. Numerous other frequencies appear for largest values of initial conditions $\dot{d}(0)$. These could be atributed to the coupling between $d(t)$ and $\sigma(t)$ and nonlinearity of the system.

2. Now we are going to investigate the case when the initial conditions are: $\dot{\sigma}(0) \neq 0$ and $\dot{d}(0) = 0$.

   In this case, there are no oscillations of $d(t)$. Let us have a look at the oscillations of $\sigma(t)$, for the different values of $\dot{\sigma}(0) = 0.001,\ 0.005,\ 0.01,\ 0.05,\ 0.1,\ 0.5$, in figures 4.6 and 4.7.

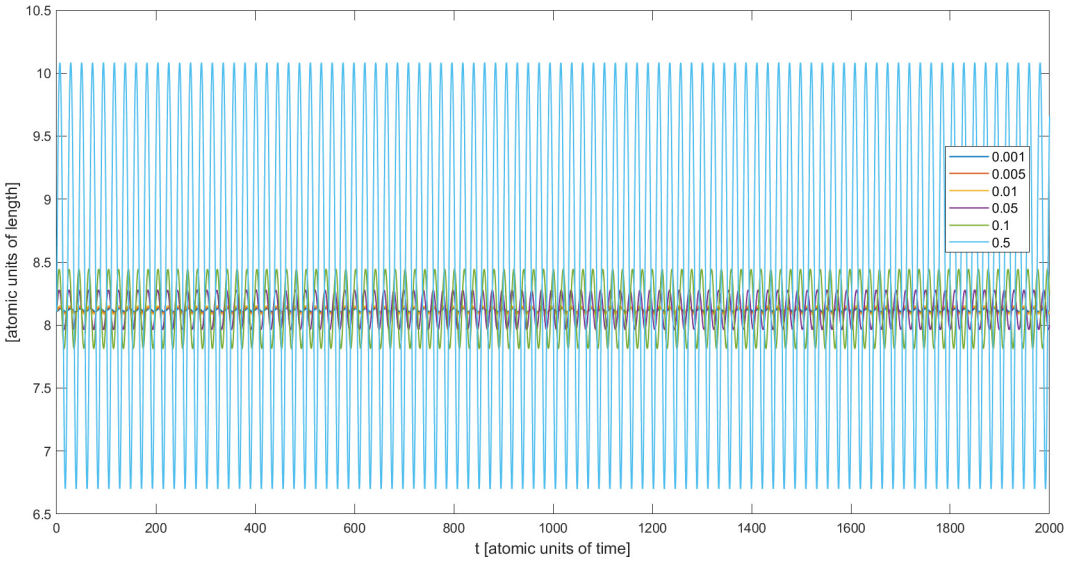

Figure 4.6: Amplitude of oscillations of $\sigma(t)$ in atomic units for different values of $\dot{\sigma}(0)$

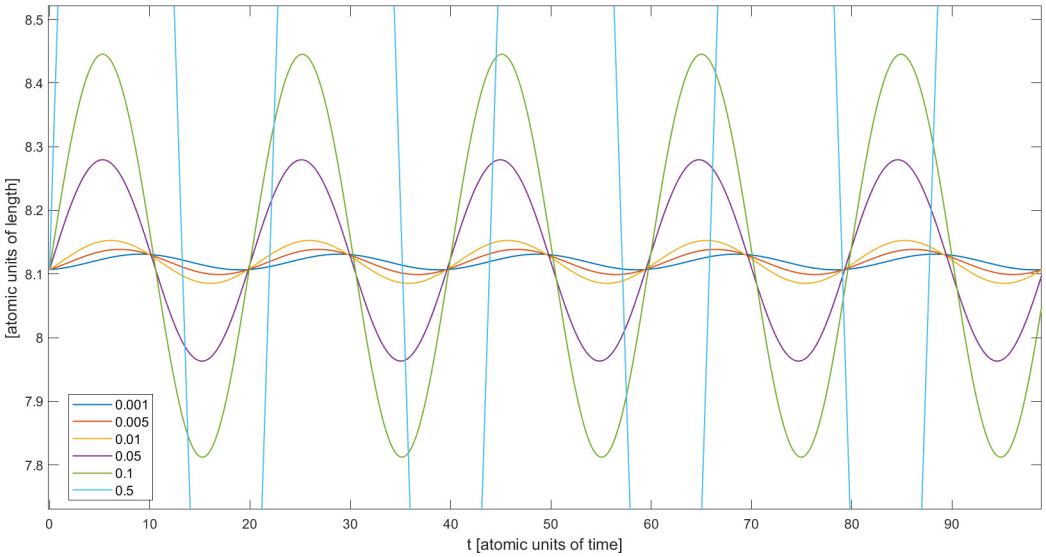

Figure 4.7: Amplitude of oscillations of $\sigma(t)$ in atomic units for different values of $\dot{\sigma}(0)$, zoomed in for better clarity

As we can see, not only does the amplitude of oscillations increase for larger values of initial conditions, there is also a change in frequency of oscillations. For increasing values of initial conditions, the frequency of oscillations decreases, as can be seen using the fast Fourier transform in figure 4.8.

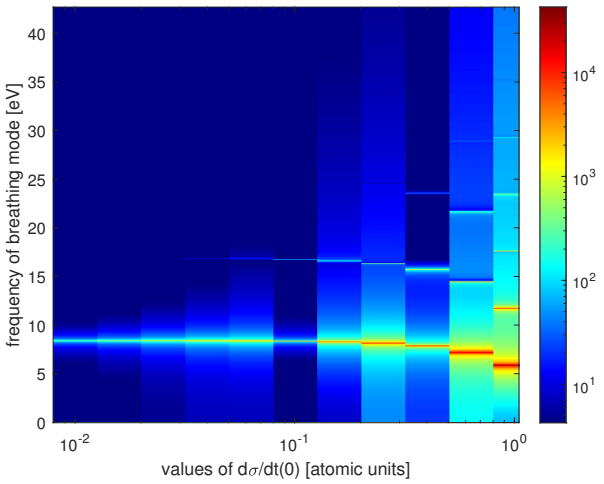

Figure 4.8: Frequency of oscillations of $\sigma(t)$ (breathing mode) depending on different values of $\dot{\sigma}(0)$

This shows that the oscillator is indeed anharmonic, which is caused by the non-parabolic shape of the pseudopotential $U(\sigma)$. Therefore, the frequency is a function of amplitude. In the figure 4.8, we can also see higher harmonics appearing for larger values of initial conditions.

Chapter 5

Applying alternating external electric field

So far, we have been investigating cases, when we are able to excite a specific initial value of either $\dot{d}(0)$ or $\dot{\sigma}(0)$. Now, we are going to excite our system using an alternating external electric field along the z-axis, with amplitude E_0 and frequency ω. The initial values will be $\dot{d}(0) = \dot{\sigma}(0) = 0$. We are also going to introduce a phenomenological damping and investigate how this affects our system. The equations of motion will therefore be modified:

$$\ddot{d} = -{\Omega_d}^2(\sigma)d + 4K(\sigma)d^3 + E_0 \sin(\omega t) - \gamma_d \dot{d}, \tag{5.1}$$

$$\ddot{\sigma} = \frac{1}{M(a)}\left[-\frac{dU(\sigma)}{d\sigma} - \Omega_d(\sigma)\frac{d\Omega_d(\sigma)}{d\sigma}d^2 + \frac{dK(\sigma)}{d\sigma}d^4 \right] - \gamma_\sigma \dot{\sigma}. \tag{5.2}$$

The value of phenomenological damping was chosen to be $\gamma_d = \gamma_\sigma = \gamma = 0.01375$ [3, 9–11]. We are going to investigate two different instances: $\omega = 0.03675\,\mathrm{AU}$ (corresponds to 1ėV in the electromagnetic spectrum), which was chosen as an arbitrary frequency in the visible region of the electromagnetic spectrum, and $\omega = \Omega_d(\sigma_0) = 0.2663\,\mathrm{AU}$ (corresponds to 7.246 eV in the electromagnetic spectrum), which is the resonant frequency of the oscillation of $d(t)$. We are going to vary the value of E_0.

5.1 Frequency of external electric field in the visible region of the electromagnetic spectrum

Firstly, we are going to investigate the case when the frequency of the external electric field corresponds to 1 eV.

- oscillations of $d(t)$

  1. **no damping**

If the damping $\gamma = 0$, there are two oscillation frequencies present for the oscillation of $d(t)$ - the oscillation frequency of the external electric field and the resonant frequency of $d(t)$, as can be seen in figures 5.1 and 5.2. The oscillation frequency of the external electric field is dominant, as we are using the initial condition $\dot{d}(0) = 0$.

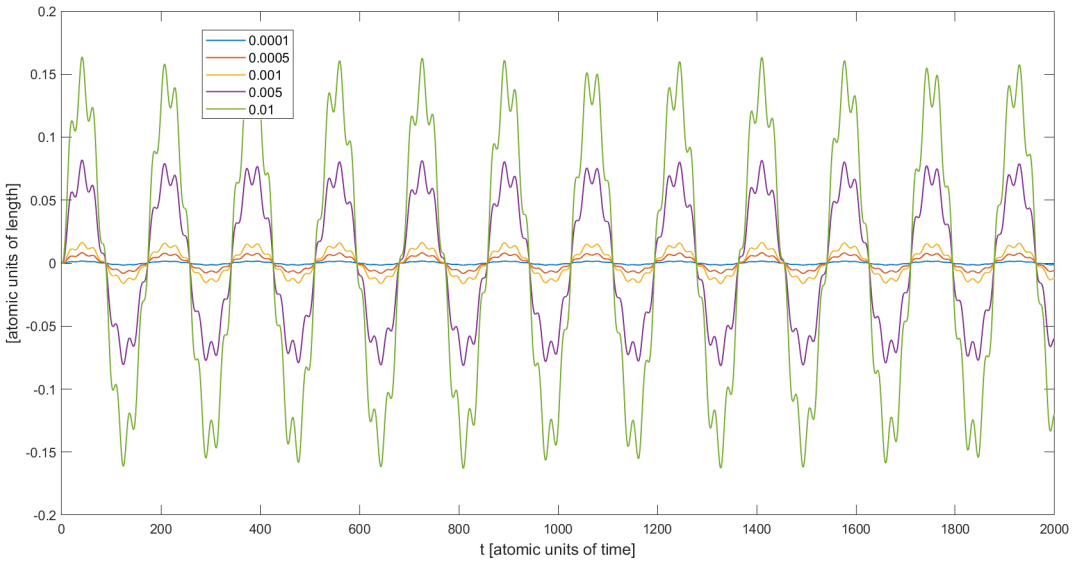

Figure 5.1: Amplitude of oscillations of $d(t)$ in atomic units depending on different values of E_0, no damping

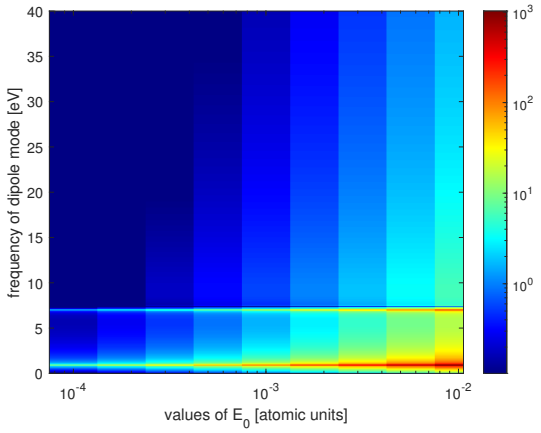

Figure 5.2: Frequency of oscillations of $d(t)$ depending on different values of E_0, no damping

2. **damping applied**

   When damping is applied, the effect of the resonant frequency of $d(t)$ is only present at the very beginning and is then extinguished by the damping (figure 5.3). In figure 5.4, we can see a very faint line at the

resonant frequency of $d(t)$, which would not even be present if we only investigated the oscillations after the initial transient phase.

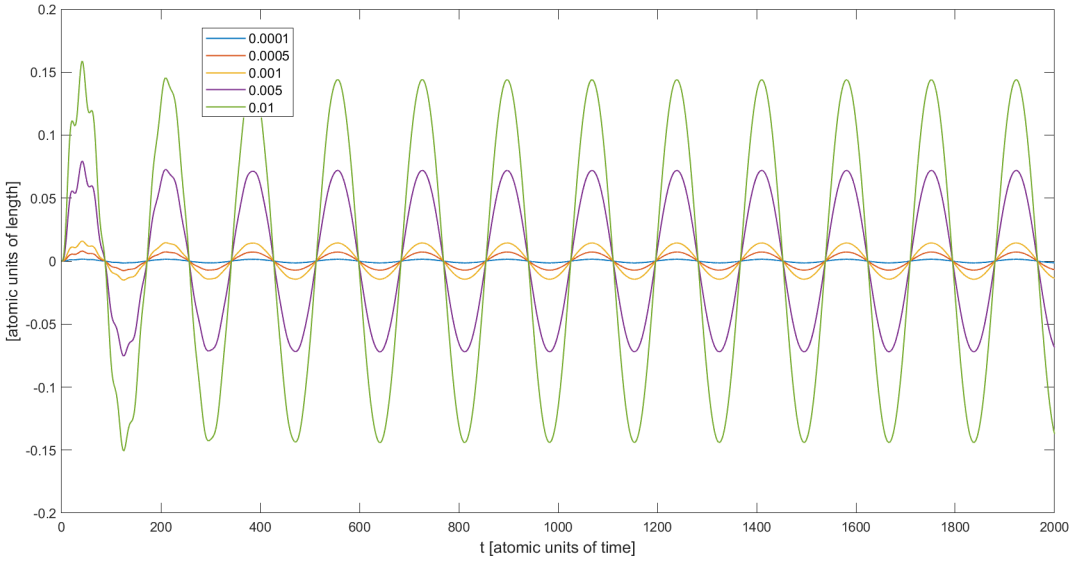

Figure 5.3: Amplitude of oscillations of $d(t)$ in atomic units depending on different values of E_0, damping applied

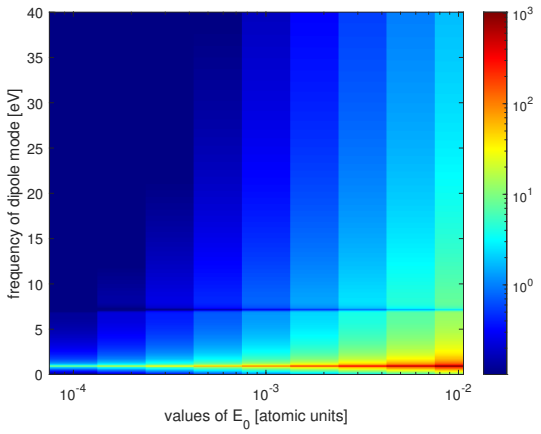

Figure 5.4: Frequency of oscillations of $d(t)$ depending on different values of E_0, damping applied

- oscillation of $\sigma(t)$:

  1. **no damping**

     Unlike for the oscillation of $d(t)$, there is mainly the resonant frequency of $\sigma(t)$ present for the oscillation of $\sigma(t)$. The frequency of the external electric field starts to have a very faint effect only for the largest values of E_0 (figure 5.7). Therefore, we can conclude, that for smaller values of E_0, the external electric field doesn't affect the oscillation of the breathing

mode. For large values of E_0, we can notice a faint line at frequency 2ω, which is due to the nonlinearity of our equations.

Furthermore, we can notice the same effect as in chapter 4 when investigating eigenoscillations of $\sigma(t)$: the amplitude of the oscillations is constant for different values of E_0 and there is an overall shift of the equilibrium value of oscillations towards a value which is slightly larger that σ_0.

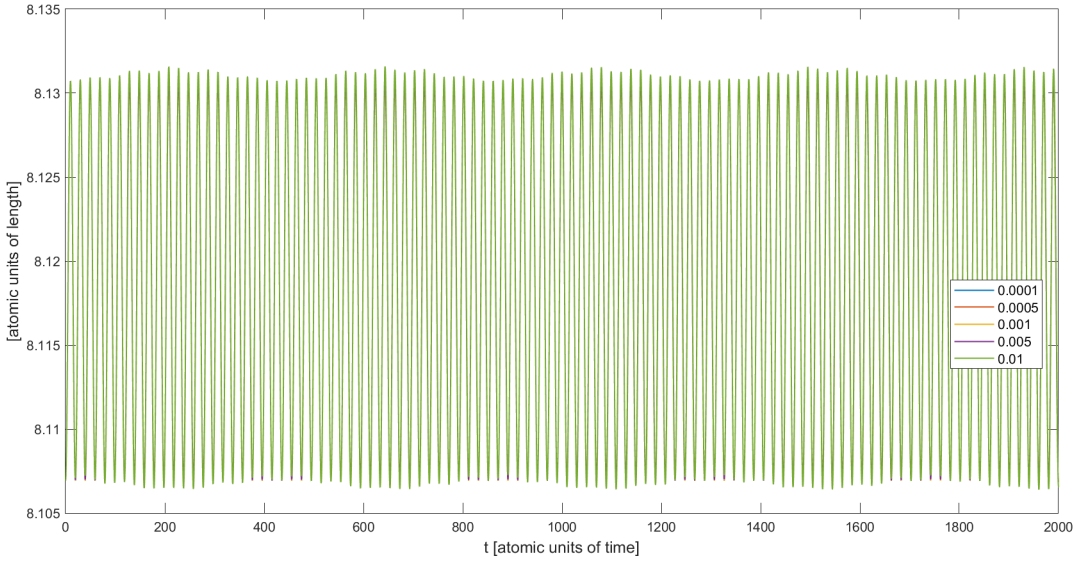

Figure 5.5: Amplitude of oscillations of $\sigma(t)$ in atomic units depending on different values of E_0, no damping

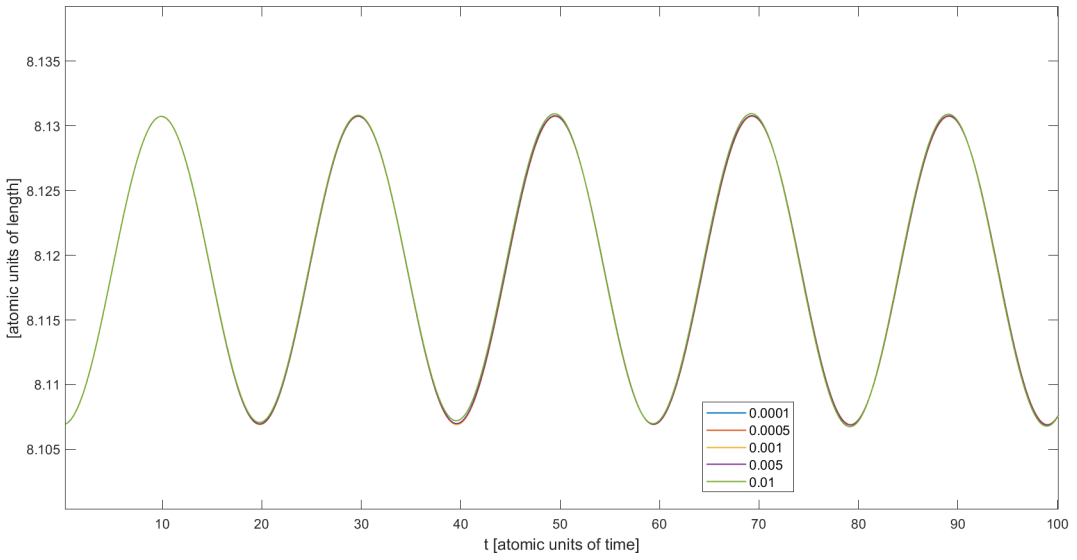

Figure 5.6: Amplitude of oscillations of $\sigma(t)$ in atomic units depending on different values of E_0, no damping, zoomed in for better clarity

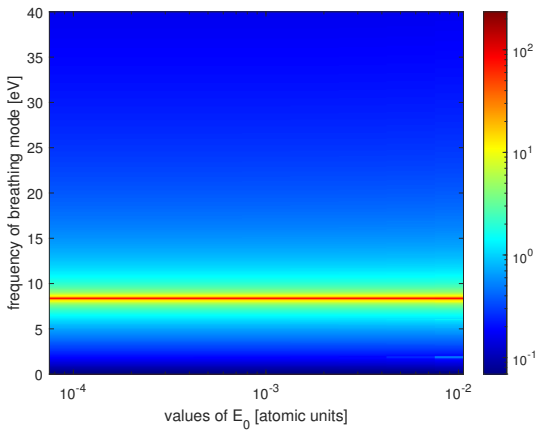

Figure 5.7: Frequency of oscillations of $\sigma(t)$ depending on different values of E_0, no damping

2. **damping applied**

   After applying damping, we can observe a continuous decrease in amplitude of oscillations of $\sigma(t)$ (figures 5.8, 5.9). Similarly to the case of no damping, the dominant oscillation frequency is the resonant frequency of $\sigma(t)$. For larger values of E_0, we can see the effect of the external electric field, at frequency 2ω (figure 5.10). Note that no oscillations can be observed at the excitation frequency ω.

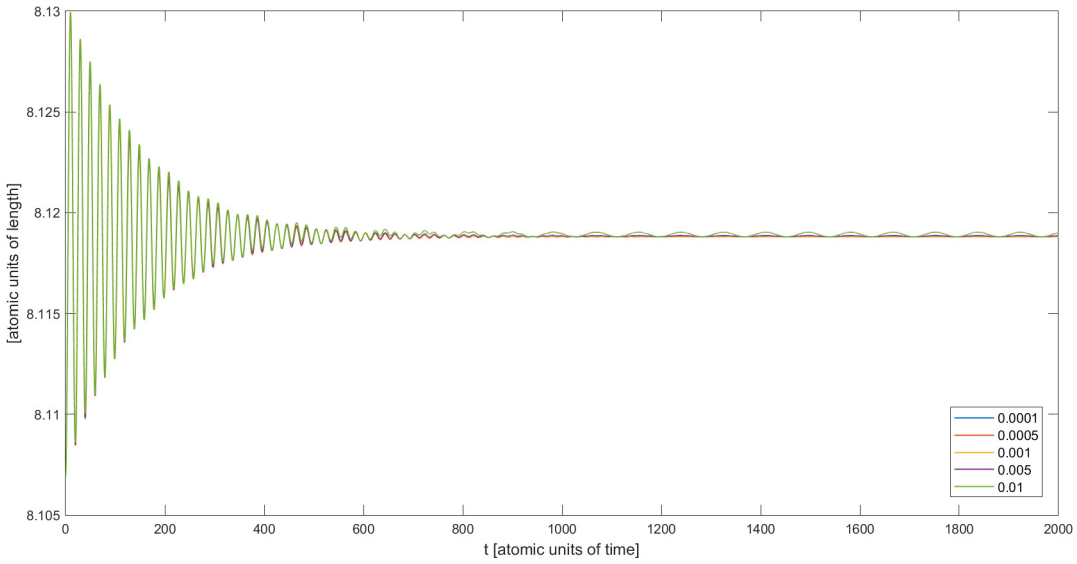

Figure 5.8: Amplitude of oscillations of $\sigma(t)$ in atomic units depending on different values of E_0, damping applied

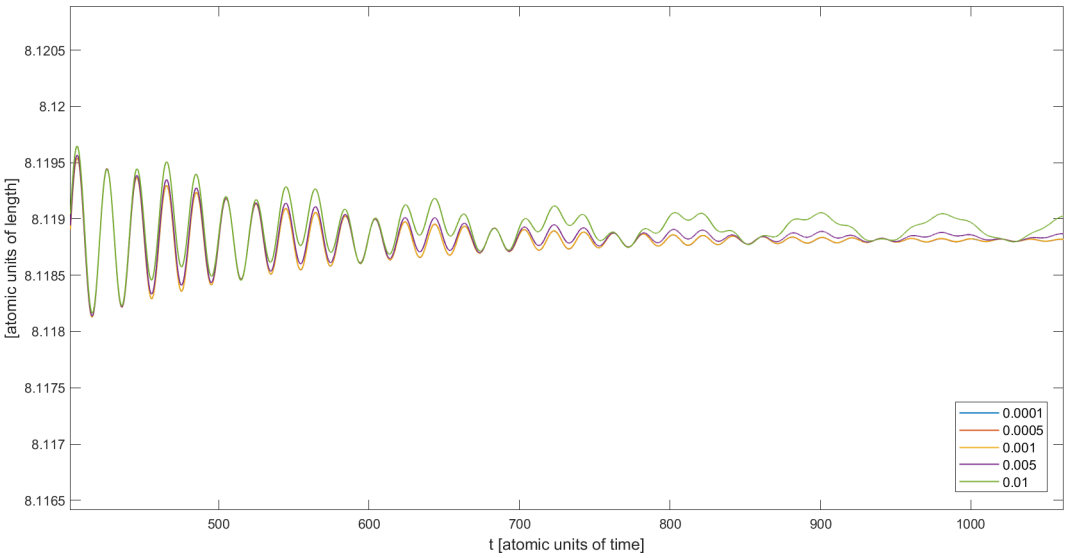

Figure 5.9: Amplitude of oscillations of $\sigma(t)$ in atomic units depending on different values of E_0, damping applied, zoomed in for better clarity

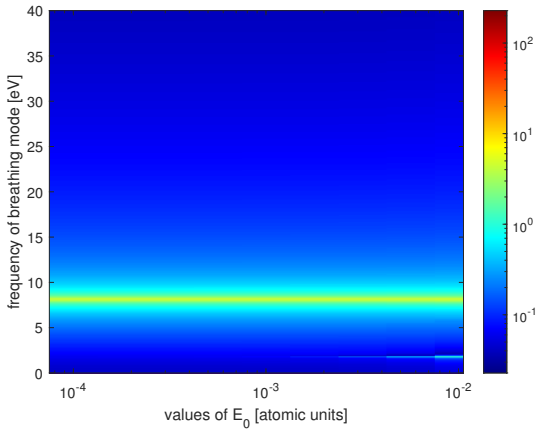

Figure 5.10: Frequency of oscillations of $\sigma(t)$ depending on different values of E_0, damping applied

From now on, we will investigate only the cases when the damping is applied.

5.2 Frequency of external electric field = resonant frequency of $d(t)$

- oscillation of $d(t)$

  When we excite the system at the resonant frequency of $d(t)$, the only frequency present for oscillations of $d(t)$ is said frequency (figure 5.12). In terms of the amplitude of oscillations, we observe two regimes (figure 5.11), which

are often referred to as the **transient regime**, in which the amplitude continuously grows and the **stationary regime**, in which the amplitude remains constant [3].

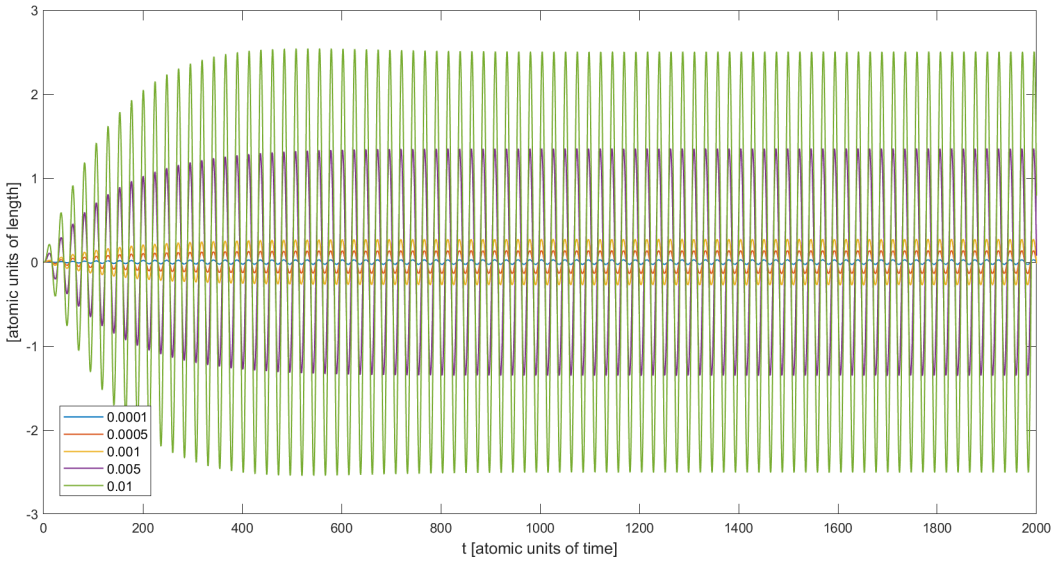

Figure 5.11: Amplitude of oscillations of $d(t)$ in atomic units depending on different values of E_0, damping applied

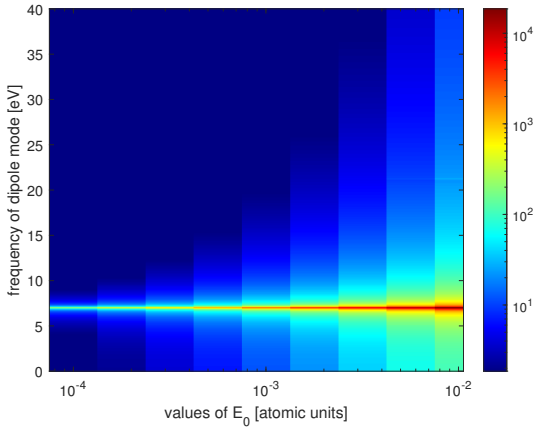

Figure 5.12: Frequency of oscillations of $d(t)$ depending on different values of E_0, damping applied

- oscillation of $\sigma(t)$

  For the oscillation of $\sigma(t)$, there are also two regimes present - the transient regime, when the amplitude of oscillations varies, and the stationary regime, when the amplitude remains constant (figure 5.13).

  We can notice the same effect which has already been mentioned a few times - the equilibrium value of oscillations is larger than σ_0. Furthermore, this value increases for larger values of E_0.

In figure 5.14, we can see two distinct frequencies of oscillations - the resonant frequency of $\sigma(t)$ and 2ω.

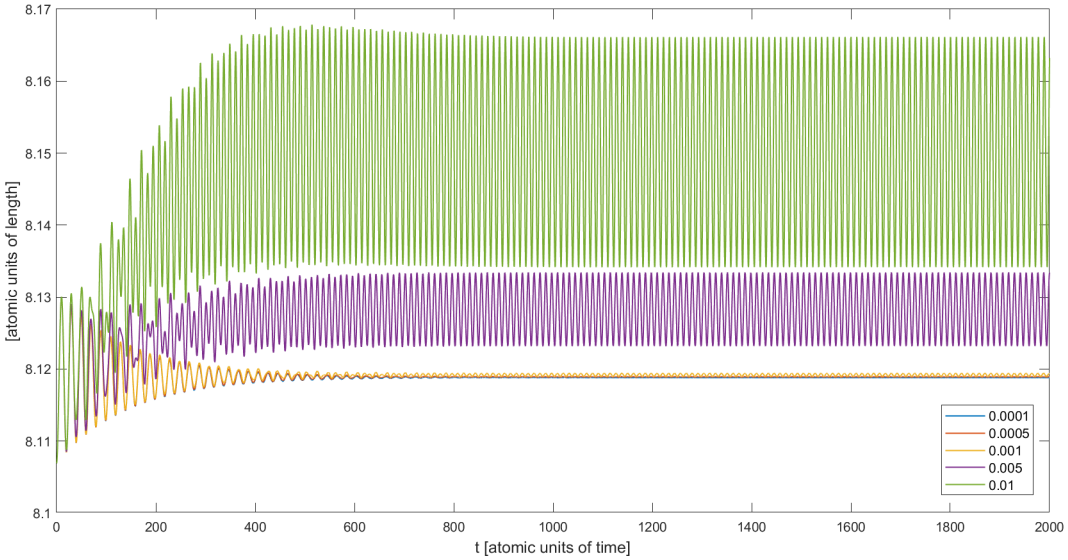

Figure 5.13: Amplitude of oscillations of $\sigma(t)$ in atomic units depending on different values of E_0, damping applied

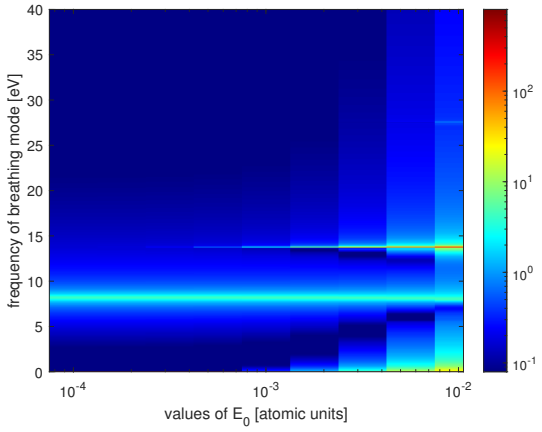

Figure 5.14: Frequency of oscillations of $\sigma(t)$ depending on different values of E_0, damping applied

Chapter 6

Electronic current density

Now that we have solved the equations describing our system and determined the oscillations of $d(t)$ and $\sigma(t)$, we are able to calculate and plot the spatial distribution of the electronic current density $\mathbf{j} = n\mathbf{u}$ [3]:

$$\mathbf{j}(\mathbf{r},t) = n(\mathbf{r},t)\mathbf{u}(\mathbf{r},t) = n(\mathbf{r},t)\left(\frac{\dot{\sigma}}{\sigma}x\hat{\mathbf{x}} + \frac{\dot{\sigma}}{\sigma}y\hat{\mathbf{y}} + \left[\frac{\dot{\sigma}}{\sigma}(z-d) + \dot{d}\right]\hat{\mathbf{z}}\right), \tag{6.1}$$

where we used the already derived expression for mean electron velocity $\mathbf{u}$ (2.4). The parameters used in this chapter are:

$$\begin{aligned} R &= 1 \text{ nm} \\ E_0 &= 0.001 \text{ AU} \\ \omega &= 1\text{eV} \\ \gamma &= 0.01375. \end{aligned}$$

We are investigating the case when the frequency of the exciting electric field is in the visible region of the electromagnetic spectrum and damping is applied to both dipole and breathing mode. First, let us have a look at the oscillations of these modes and their time derivatives in figure 6.1:

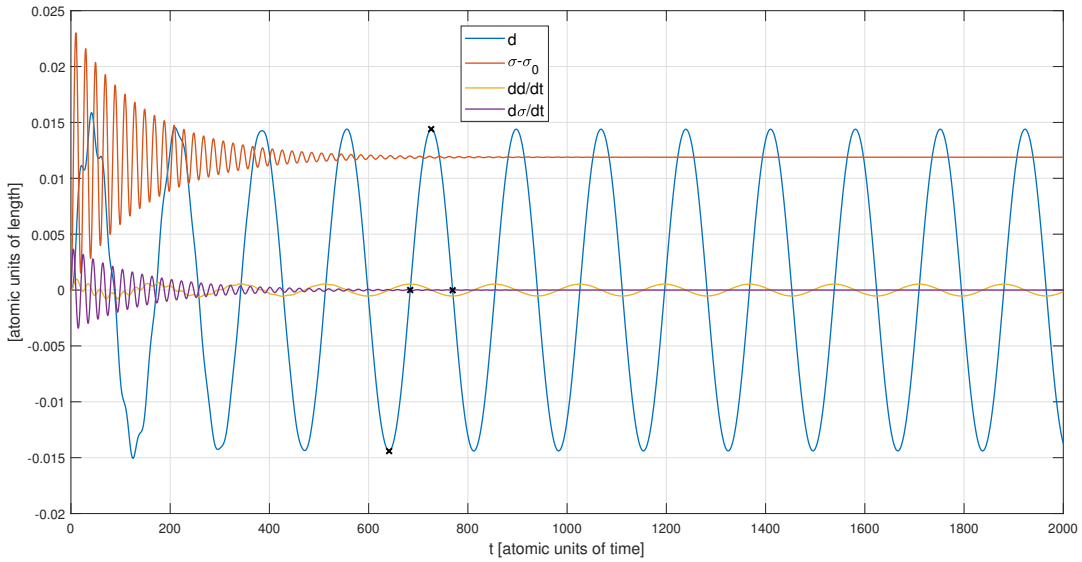

Figure 6.1: Oscillations of $d(t)$, $\sigma(t)$, $\dot{d}(t)$ and $\dot{\sigma}(t)$ for nonzero damping γ, $E_0 = 0.001\,\mathrm{AU}$, $\omega = 1\,\mathrm{eV}$

We investigate four distinct points in time, denoted by black crosses. At $t = 641.3\,\mathrm{AU}$ and $t = 726.7\,\mathrm{AU}$ (first and third black cross), $d(t)$ is maximal, therefore $\dot{d}(t) = 0$. We can visualize the breathing mode at these two points in time. At $t = 683.9\,\mathrm{AU}$ and $t = 769.4\,\mathrm{AU}$ (second and fourth black cross), $d(t) = 0$, therefore $\dot{d}(t)$ is maximal and the dipole mode can be visualized at these two points in time (breathing mode is also present).

The four following graphs in figures 6.2 and 6.3 show a cross-section of the vector field $\mathbf{j}(\mathbf{r}, t)$ in the plane (x,z), where y=0, for the four chosen points in time:

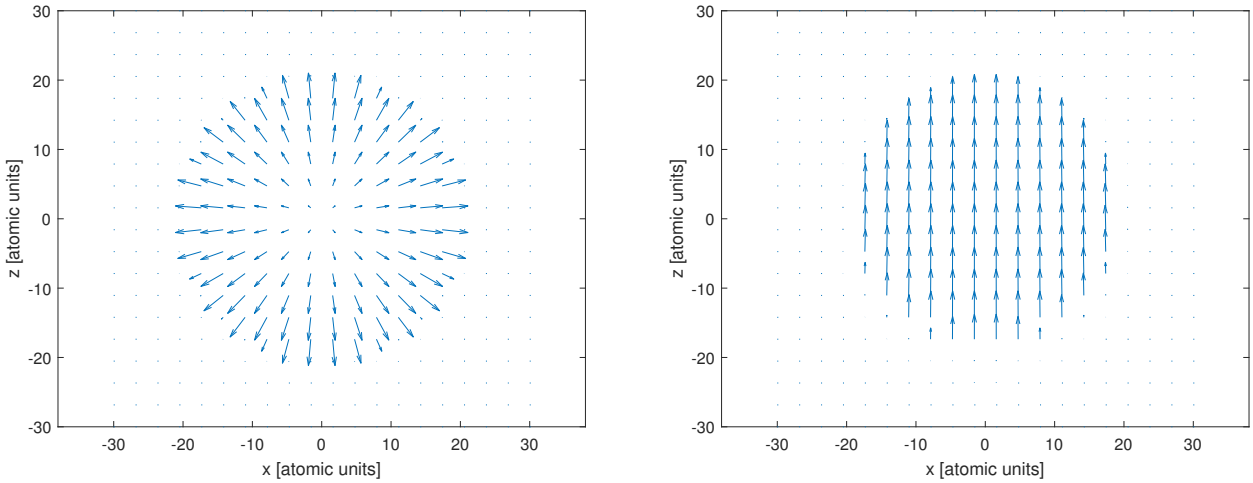

Figure 6.2: Cross-section of $\mathbf{j}(\mathbf{r}, t)$ in the (x,z) plane [atomic units of length] for $t = 641.3\,\mathrm{AU}$ and $t = 683.9\,\mathrm{AU}$, respectively

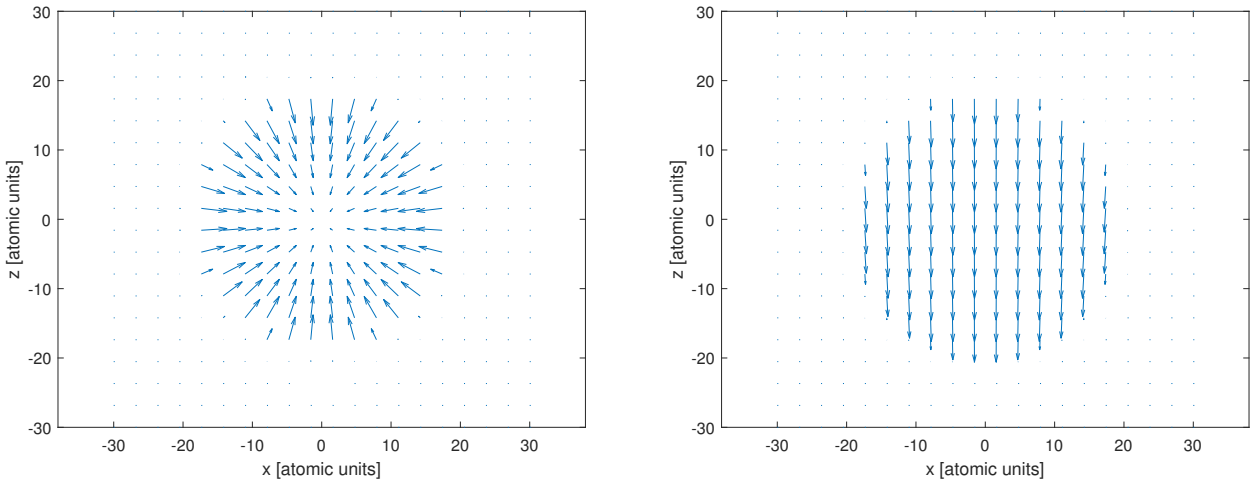

Figure 6.3: Cross-section of $\mathbf{j}(\mathbf{r}, t)$ in the (x,z) plane [atomic units of length] for $t = 726.7\,\mathrm{AU}$ and $t = 769.4\,\mathrm{AU}$, respectively

Note that the scale of current density represented by arrows is different in each figure.

Now, corresponding to each of the four graphs for the four chosen points in time, we can graph the z-component of the current density $\mathbf{j}$ depending on the z-component in space:

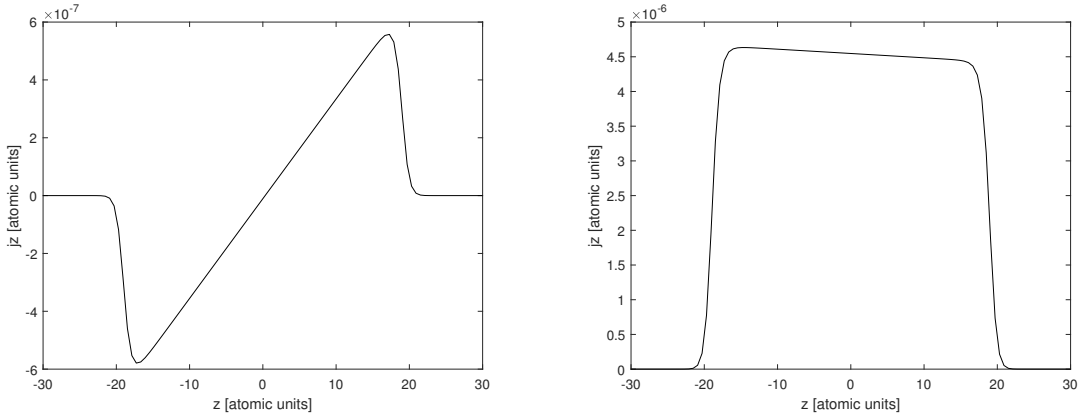

Figure 6.4: j_z depending on z-component in space [atomic units], for $t = 641.3\,\mathrm{AU}$ and $t = 683.9\,\mathrm{AU}$, respectively

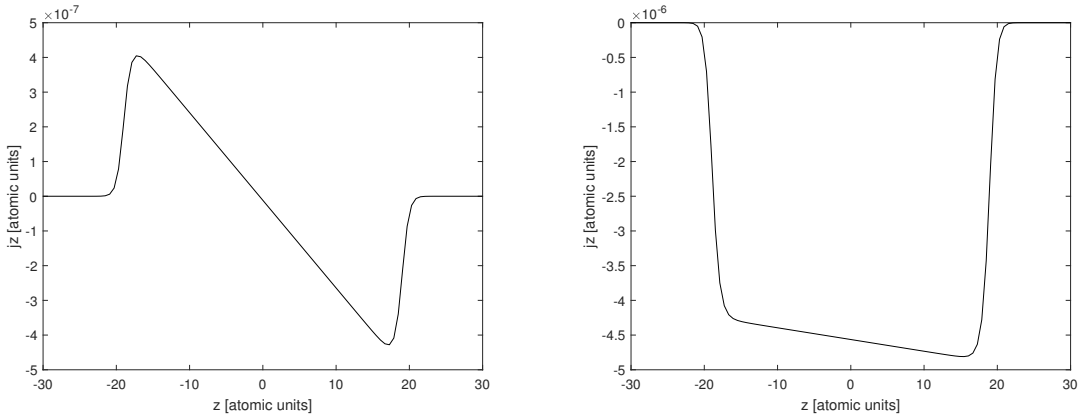

Figure 6.5: j_z depending on z-component in space [atomic units], for $t = 726.7\,\mathrm{AU}$ and $t = 769.4\,\mathrm{AU}$, respectively

The graphs on the left in figures 6.4 and 6.5 correspond to the radial current of the breathing mode, the graphs on the right correspond to the dipole mode. The linear slant of the slope of the current density j_z inside the nanoparticle is due to the nonzero radial current. From these graphs, we can determine the width of the interface region close to the surface of the nanoparticle, in which the current density gradually transitions to zero. For the dipole mode, this layer was determined to occupy the interval $(R - 0.1\mathrm{nm}, R + 0.1\mathrm{nm})$ (figure 6.6):

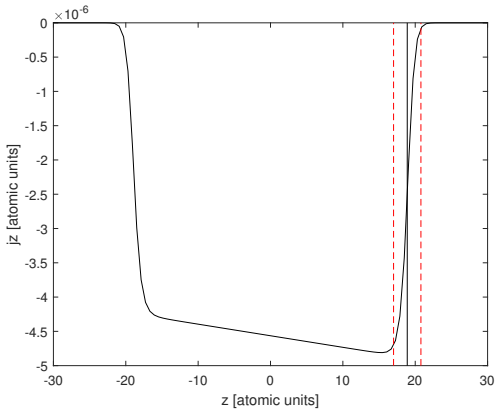

Figure 6.6: j_z depending on z-component in space [atomic units], for $t = 769.4\,\mathrm{AU}$

Conclusion

In this thesis, we investigate dynamics of electrons inside a golden nanoparticle. We start with the Lagrangian density, from which we derive the QHD (Quantum hydrodynamic) equations. Furthermore, we choose an expected solution (ansatz) for the electron density, which we insert into the Lagrangian density. The Lagrangian density is then integrated over space in order to obtain the Lagrangian.

Using the Euler-Lagrange method, we derive equations with two dynamic variables $d(t)$ (displacement of center of mass of the electrons relative to fixed ion background) and $\sigma(t)$ (spillout of the electrons at the surface of nanoparticle). Moreover, we determine the value of the spillout of the ground state σ_0 and find out that the choice of number of electrons per atom has minimal impact on the value of the ground state σ_0.

We numerically solve the equations with dynamic variables $d(t)$ and $\sigma(t)$ using the Runge-Kutta method. We investigate different cases of the initial conditions of the equations. Furthermore, we use an alternating external electric field to excite our system, while also including damping. We investigate two different values of frequency of the external field, one in the visible region of the electromagnetic spectrum and one corresponding to the resonant frequency of the dipole mode.

We visualize the oscillations of $d(t)$ and $\sigma(t)$ and using the fast Fourier transform, we determine the frequencies of their oscillations. The resonant frequency of the dipole mode is determined to correspond to $\Omega_d(\sigma_0) = 7.2\,\mathrm{eV}$, for breathing mode, it is $8.3\,\mathrm{eV}$. When investigating the breathing mode, we noticed another frequency present apart from the resonant frequency of $\sigma(t)$. If we use the initial condition $\dot{d}(0)$, frequency $2\Omega_d(\sigma_0)$ appears. If we use external electric field with oscillation frequency ω to excite our system, frequency 2ω appears.

Additionally, we notice an interesting phenomenon for the oscillation of $\sigma(t)$. The equilibrium value around which $\sigma(t)$ oscillates, is not equal to the ground state σ_0, rather slightly larger. We also find that this equilibrium value depends on the excitation conditions of our system. For increasing values of the amplitude of the external field E_0, the equilibrium value also increases.

Finally, we use the numerical solutions of $d(t)$ and $\sigma(t)$ to calculate and plot the electronic current density. We visualize the dipole and the breathing mode and determine the width of the interface region at the surface of the nanoparticle, in which the current density gradually transitions to zero.

References

[1] J. D. Patterson and B. C. Bailey, *Solid-state physics: introduction to the theory*. Springer Science & Business Media, 2007.

[2] D. Michta, F. Graziani, and M. Bonitz, "Quantum hydrodynamics for plasmas–a thomas-fermi theory perspective," 2015.

[3] J. Hurst, P. M. Oppeneer, G. Manfredi, and P.-A. Hervieux, "Magnetic moment generation in small gold nanoparticles via the plasmonic inverse faraday effect," *Physical Review B*, vol. 98, no. 13, p. 134439, 2018.

[4] J. Hurst, F. Haas, G. Manfredi, and P.-A. Hervieux, "High-harmonic generation by nonlinear resonant excitation of surface plasmon modes in metallic nanoparticles," *Physical Review B*, vol. 89, no. 16, p. 161111, 2014.

[5] L. N. Hand and J. D. Finch, *Analytical mechanics*. Cambridge University Press, 1998.

[6] C. Johnson, *Numerical solution of partial differential equations by the finite element method*. Courier Corporation, 2012.

[7] H. King, "Crystal structures and lattice parameters of allotropes of the elements," *CRC Handbook of Chemistry and Physics*, pp. 15–18, 2016.

[8] V. S. Ryabenkii and S. V. Tsynkov, *A theoretical introduction to numerical analysis*. Chapman and Hall/CRC, 2006.

[9] A. Derkachova, K. Kolwas, and I. Demchenko, "Dielectric function for gold in plasmonics applications: size dependence of plasmon resonance frequencies and damping rates for nanospheres," *Plasmonics*, vol. 11, no. 3, pp. 941–951, 2016.

[10] A. Brandstetter-Kunc, G. Weick, D. Weinmann, and R. A. Jalabert, "Erratum: Decay of dark and bright plasmonic modes in a metallic nanoparticle dimer [phys. rev. b 91, 035431 (2015)]," *Physical Review B*, vol. 92, no. 19, p. 199906, 2015.

[11] X. Li, D. Xiao, and Z. Zhang, "Landau damping of quantum plasmons in metal nanostructures," *New Journal of Physics*, vol. 15, no. 2, p. 023011, 2013.